Anti- and de-icing methods for rotorcraft applications: a critical review

Patnaik, P.C.; Sarda, K.; Leung, W.; Carignan, S.; Oleskiw, M.

Publisher's version / Version de l'éditeur:
https://doi.org/10.4224/23000207
Laboratory Technical Report (National Research Council of Canada. Institute for Aerospace Research. Structures and Materials Performance Laboratory); no. LTR-SMPL-2004-0175, 2004-08-17

National Research Council Canada
Conseil national de recherches Canada

Institute for Aerospace Research
Institut de recherche aérospatiale

Unclassified
Unlimited

NRC·CNRC

Anti- & De-Icing Methods for Rotorcraft Applications: A Critical Review

LTR-SMPL-2004-0175

P.C. Patnaik, K. Sarda, W. Leung, S. Carignan and M. Oleskiw

August 2004

Canada

INSTITUTE FOR
AEROSPACE RESEARCH

REPORT
RAPPORT

INSTITUT DE RECHERCHE
AÉROSPATIALE

Report No.: LTR-SMPL-2004-0175

Date: 17 August 2004

Classification: Unclassified
Distribution: Unlimited

Pages: 59

Tables: 19

Figures: 27

STRUCTURES, MATERIALS AND
PROPULSION LABORATORY

LABORATOIRE DES
STRUCTURES, DES MATÉRIAUX
ET DE PROPULSION

For:
Pour:

Reference:
Référence:

LTR-SMPL-2004-0175

Anti- & De-Icing Methods for Rotorcraft Applications: A Critical Review

Submitted by:
Présenté par: J.P. Komorowski
Director/Directeur

Approved by:
Approuvé par: D.L. Simpson
Director General/Directeur général

Author(s):
Auteur(s): P.C. Patnaik
K. Sarda
W. Leung
S. Carignan
M. Oleskiw

Anti- & De-Icing Methods for Rotorcraft Applications: A Critical Review

Prakash C. Patnaik *
Karan Sarda *
Wayne Leung *
Stephan Carignan **
Myron Oleskiw ***

* Structures, Materials & Propulsion Laboratory
Flight Research Laboratory, * Aerodynamics Laboratory
IAR-NRC, Ottawa

Executive Summary

In-flight and ground icing has historically posed a significant problem for all types of aircraft, and has been determined to be the cause of numerous accidents. Canadian airspace is especially hazardous as air temperatures are typically sub-zero, leading to ripe conditions for the onset of icing. Ice accretion on the leading edge and other areas of wings, fuselage, windows, engine inlets, and sensors degrade the aerodynamic form of the aircraft, and results in decreased lift and a higher stall velocity. Multiple solutions to this problem have been developed and applied to fixed-wing and, to a lesser extent, rotary aircraft. Most of these applications have shown promise and some have already seen limited service time. However, all current applications have considerable disadvantages, specifically in terms of weight and power requirements.

Rotorcraft are known to be particularly sensitive to in-flight icing due to the large effective distance the rotor blades travel compared to the effective distance that any component of a fixed-wing aircraft travels. The lift generated by the rotor blades is extremely sensitive to the effective shape of the blade itself; therefore, it is imperative that ice is either prevented from forming, or effectively removed once formed.

The majority of today's civil and military helicopters certified to fly in icing conditions are equipped with electro-thermal ice protection systems. Due to their proven record of reliability, durability and effectiveness versus the complete spectrum of other de-icing technologies developed, electro-thermal de-icing remains the favored solution after decades of research and development. However, due to the weight and considerable power consumption demands of an electro-thermal system, alternate anti- and de-icing methods have been intensely studied. This paper summarizes the numerous anti-/de-icing methods that have been studied and/or applied to rotorcraft to replace the electro-thermal systems and explores the feasibility of using shape memory alloy actuated systems as a more efficient means of rotorcraft de-icing.

Table of Contents

List of Figures

List of Tables

1.0 Introduction

Aircraft icing has been a problem that has plagued aviators since the dawn of aviation. Frigid atmospheric temperatures as aircraft pass through clouds produce conditions favorable to the onset of ice formation on the fuselage, wings or, in the case of rotorcraft, the rotor blades. As the formation of ice alters the airfoil shape, aircraft performance degrades; lift is lost, drag increases and stall speed increases. Asymmetrical flight characteristics experienced in rotorcraft due to the varying ice formations accumulated on different blades induce severe vibrations which could potentially damage the gearbox, drive train and airframe or result in a loss of flight stability. In order to provide full icing capabilities, protection must be provided to engine intakes, windscreens, aerials, and wings. However, it is rotor blades that present the greatest design challenge.

Protection systems can be divided into two categories: *anti-icing systems* which prevent any icing formation, or *de-icing systems* which act to de-bond existing ice formations. To date, the electro-thermal anti-/de-icing systems remain the favored solution, and are employed on most military and civilian aircraft currently certified to fly in icing conditions. The excessively high-energy requirements of electro-thermal protection systems have lead researchers to develop economical and practical de-icing systems. In the search for new helicopter de-icing systems, the following goals have been established:

a) Low power input
b) Low gross weight
c) Sufficient sand and erosion resistance properties
d) Aerodynamically non-intrusive design, and
e) Cost efficiency

The mechanical and thermal systems currently employed are not economically efficient, while existing chemical systems are ineffective, as films exhibit poor weathering capabilities and typically shear off once the aircraft is airborne.

Systems can be designed intrinsically into the airfoil to eliminate aerodynamic effects, or can be bonded to existing airfoils as retrofit applications. In designing a helicopter ice protection system, the following issues must to be taken into account:

a) Chord-wise and span-wise extent of ice formation
b) Rate at which ice accretes on the blades

c) Type of ice which forms
d) Degree of aerodynamic degradation
e) Airfoil shape and structure
f) Electric power capacity
g) Transmission of power from fixed base to rotating blades
h) Ice detection and warning systems
i) Power systems and pilot interfaces

Prior to the design phase, a good knowledge base on the mechanics of adhesion characteristics of the ice/substrate interface bond must be established either by testing or by literature study. Without this knowledge, realistic design requirements will not be known, possibly leading to another impractical, and unsuccessful strategy.

In the event of icing the greatest threat to rotorcraft flight safety is the degradation of aerodynamic flows. Water droplets exist in the atmosphere in a super-cooled liquid state at temperatures as low as -40°C and are formed by condensation of water vapor onto airborne particles such as dust and pollutants. The droplets remain in this super-cooled liquid state until an event such as a passing of an aircraft disturbs this equilibrium state allowing ice crystals to nucleate on the aircraft surface [1,2]. Ice formation would increase the weight and induce drag causing the rotorcraft to experience a torque rise and loss of lift, ultimately resulting in performance losses. Further problems upon the onset of icing are associated with shedding. If ice shedding is asymmetrical, large strains concentrate on the gearbox, producing dangerous vibrations and control difficulties. Asymmetrical shedding is a severe problem due to the statistical variation of adhesive strength along the ice/substrate bond, and possible partial failure of de-icing system components leave some blades able to de-ice and others not.

Ice can form in diverse densities and configurations and, as a result, the mechanical properties vary considerably. It is therefore necessary to determine and differentiate between these types of ice. Several types of ice produced and observed in icing tests are discussed below [1,3].

a) Wind tunnel ice: Substrate is cooled below the freezing point of water; water is then sprayed onto the substrate. Size and droplet momentum can be controlled by this approach.
b) Natural ice: Ice formation on a substrate is exposed to the atmosphere under natural occurring conditions.

c) Rime ice – Figure 1a, 1e: A non-homogenous phase consisting of powdery shaped particles; Super-cooled water droplets freeze immediately upon impact, trapping air beneath the surface which attributes to the distinct white appearance. Normally, rime ice accretes onto the leading edge and acts as an extension to the leading edge. High surface roughness increases drag, resulting in early boundary layer separation promoting blade stall. Rime ice is the most frequently reported ice type [21]. It is formed between temperature ranges between -40°C and -15°C, $\rho = 880\ kg/m^3$.

d) Glazed ice – Figure 1b, 1e: A homogeneous transparent hard solid phase of ice. Causes significant drag increase and lift losses, as horn shapes grow if icing encounter is sufficiently long; Water flows along blade before freezing. Ice is formed between temperature ranges from -10°C to 0°C, $\rho = 917\ kg/m^3$ (no trapped air within body).

e) Mixed ice - Figure 1c: Glazed ice surrounded by finger-like shaped rime ice. Shapes will depend on ambient temperature, liquid water content (LWC), airspeed, altitude, etc. It forms between –10°C and -15°C.

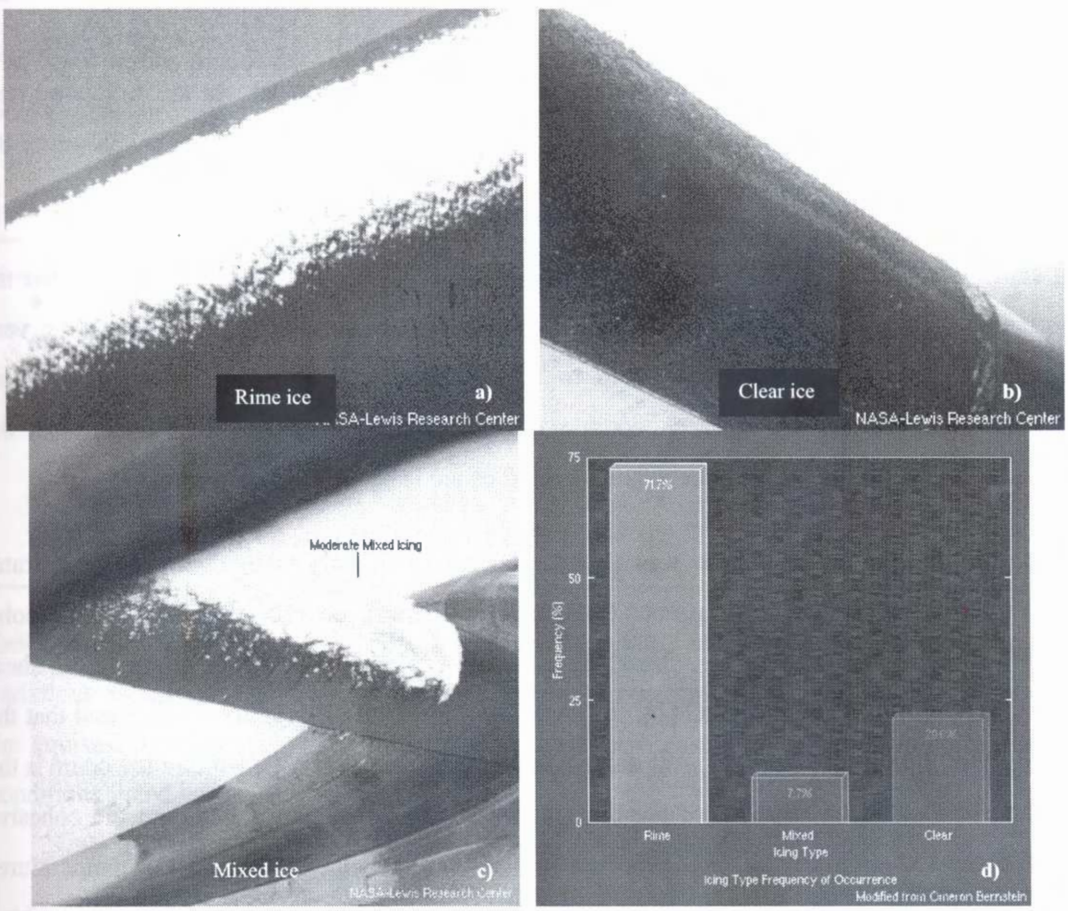

Figure 1. Typical ice formations: a) Rime ice b) Glaze or clear ice c) Mixed ice d) Icing type frequency of occurrence. [21]

Water impingement rates theoretically dictate the location of ice formation, and therefore would likely predict that the outboard span of the rotor blade would accumulate more ice since it effectively travels further in moist air. However, centrifugal and aerodynamic forces acting on the rotating airfoil prevent any appreciable ice formation on the outboard region. Viscous kinetic effects near the blade tip dominate the thermodynamic heat balance, hence freezing of impinged water will not occur and the ice level will decrease at outward span locations [4]. However, at temperatures lower than -10°C ice can form along the entire leading edge of the main rotor. On average, cloud ice will form from the leading edge to 15% of the mean aerodynamic chord (MAC) on the top surface, and to 25% MAC on the lower surface [5].

Extensive research has been conducted on the mechanics of ice bodies, particularly on aircraft icing, with various experimental procedures and approaches adopted to measure the mechanical properties of ice. However, due to the variation of these procedures and the inherently stochastic nature of ice, this testing has led to a wide range of values for the adhesive strengths of ice. However, the data and knowledge gained from these individual tests are not at all wasted. By analyzing data trends, significant fundamental principles can be exposed. In the following text, important and noteworthy observations and facts about ice behavior with direct relevance to the rotor blade-icing problem are discussed.

Using replicas of ice surfaces from polymer and metal coatings, Bascom et al. found that the basal planes of ice crystals were oriented parallel to the shear surface, thereby exhibiting very weak shear characteristics when compared to high tensile strength for prismatic slip. This observation, strengthened by research conducted by Scavuzzo and Chu, has shown that the predominant approach in breaking the adhesive bond of ice is by using shear forces [1].

The adhesive shear strength of ice was found to increase linearly with decreasing substrate-interface temperature to a specific point. Scavuzzo and Chu discovered that this specific point was –3.9°C: below this temperature, shear strength varies slightly. However, a maximum shear strength (150 psi) is obtained at -7°C [1]. Jellinek, Stallbrass, and Price, however, found that the ice shear strength increases linearly with decreasing temperature to -13°C, which they claim is the point where the adhesive strength of the ice/substrate bond becomes greater than the cohesive strength of ice. Other researchers also reported similar findings, claiming a range of temperatures where ice will fracture cohesively or at the ice/substrate interface. However, the point at which the adhesive strength of ice exceeds the crystalline strength of ice varies with each report.

Another researcher, Itagaki, claimed no change in shear strength at all with decreasing temperature [6]. Itagaki did claim that tensile strength increases with slower grown ice, however shear strength increases with faster grown ice [6]. Therefore the results from literature are very scattered due to the varying methods used to obtain these results.

Scavuzzo and Chu's research presented some other interesting conclusions on the adhesive shear strength, τ_a, of ice. They, along with Stallbrass and Price, found that τ_a was independent on the substrate material, ambient temperature (not substrate-interface temperature), and ice thickness. Stallbrass and Price, claimed that ice would stick to Teflon-coated objects as strongly as it would to metal objects [6].

Several researchers, including Lynch and Ludwiczak, concluded that surface roughness plays an important role in ice adhesion. A rough surface, contaminated with scratches and other surface defects, will have a greater contact surface, and therefore a greater shear stress will be needed to de-bond the ice.

The observations of Scavuzzo and Chu regarding factors that are dependant and independent of the adhesive shear strength of ice are summarized in Table 1.

Table 1. Adhesive shear strength of ice, τ_a

Factors which affect τ_a	Factors which do not affect τ_a
• Surface roughness • Wind velocity • Droplet momentum • Ice/Substrate interface temperature • Impact ice type (rime, glaze, etc) • Surface contamination (oil, rust, fingerprints)	• Material substrate • Rotation or non-rotation of specimen • Ice thickness

Researchers Miller & Bond [6] conducted rotor-icing studies specifically relating torque variations experienced by the rotor to various tunnel conditions. They concluded that torque, or the equivalent icing rate, rises linearly with time as a result of the various rotor and tunnel conditions listed below:

a) Cloud conditions, temperature, liquid water content (LWC), droplet size

b) Torque will steadily rise until shedding occurs (result of increasing ice thickness)

Their accumulated ice profiles were found to be fully repeatable, as were the torque values until shedding. The radial extent of non-shed ice proved to give repeatable results. However, shed time, location and quantity of shedding did not.

In order to obtain a valid solution to the icing problem, the mechanics of ice-substrate bond and the expected adhesive tensile and shear strength values of the ice-substrate interface need to be determined. Also, the span-wise and chord-wise extent of icing as well as the shape and rate of growth must be accurately predicted. It would be beneficial to conduct specific in-house rotor icing experiments prior to de-icing system design. This will provide an essential first step to addressing the design requirements of a rotor de-icing system.

Amidst all the scatter of the literature results, trends show that the adhesive shear strength for glaze ice is significantly higher than rime ice, the former approaching magnitudes almost twice as large as the latter [6]. Crack propagation in rime ice is faster than in glaze ice due to the high density of pores. Rime ice will fail cohesively rather than purely at the ice substrate interface [1].

2.0 Electro-thermal Ice Protection

The majority of the civil and military helicopters currently certified to fly in icing conditions are equipped with electro-thermal ice protection systems. Due to their proven record of reliability, durability and effectiveness compared to the complete spectrum of competing de-icing technologies developed, electro-thermal de-icing remains the favored solution after decades of research and development.

The principle of the electro-thermal systems is simple and can be categorized into either anti-icing or de-icing classes. In the anti-icing case, the heat is used to evaporate or prevent impingement of cloud water droplets onto the aircraft surface. The heat provided by the resistive elements maintains the surface temperatures to either evaporate the droplets upon contact, or only provide enough energy to prevent ice from freezing (known as "running wet" systems). Caution must be taken to design running wet systems, as the water may refreeze in critical locations. On the other hand, for de-icing electro-thermal systems, the heat provided is used to de-bond the formed ice caps from the surface by melting the ice at the substrate-ice interface, thereby allowing aerodynamic and centrifugal forces to sweep the ice away. Since electro-thermal de-icing systems only realistically destroy the ice substrate interface bond and rely on centrifugal and aerodynamic forces to remove the bulk ice, it is evident that the ice thickness must be at a minimum value (roughly 0.3") [4] to have effective shedding.

The following equipment is required for a typical electro-thermal system:

i. Power source – either an extraction of the aircrafts own electrical system or an auxiliary power unit
ii. Power distribution system
iii. Control system (manual or automatic)
iv. Resistive heaters
v. Temperature sensors at the heated surface

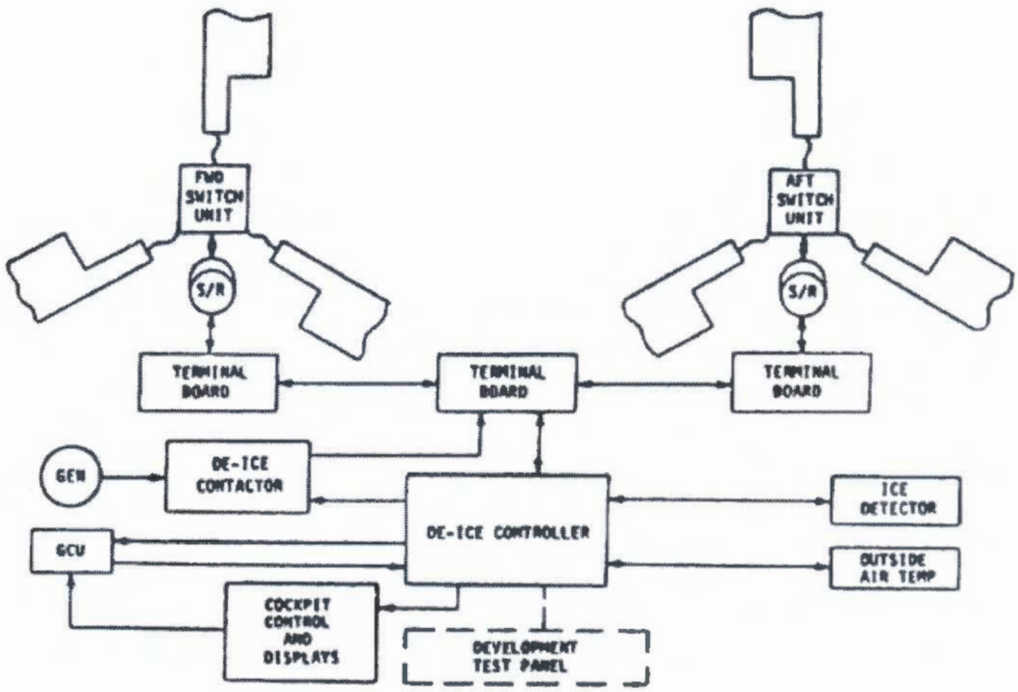

Figure 2. Schematic set-up of a rotorcraft electro-thermal de-icing system. [7]

A schematic of the set-up for an electro-thermal de-icing system is shown in Figure 2. The heater mat assembly consists of resistive elements (mat, foil, or coil format) incorporated within layers of composite material, normally fiberglass/epoxy, plastic, rubber, or metal. The heaters are typically:

a) Woven or etch foil bonded onto a carrier
b) A conductive composite material, or
c) A sprayed metallic coating

The materials chosen for the heater blanket must be resistant to rain, hail, and insect strikes, must have good fatigue and thermal limits (cyclic expansion and contraction), and adequate stress-strain properties. A dielectric layer is sprayed onto both sides of the heater mats in order to insulate them from energy loss to the erosion shield and spar. A schematic of typical heater mat assemblies is given below in Figure 3.

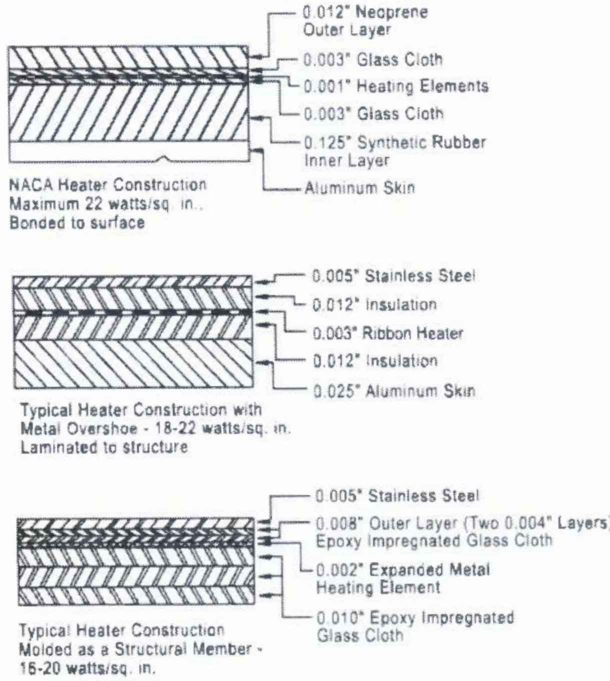

Figure 3. Three typical cross sections of electro-thermal heater elements. [7]

Typically, there are two ways of installing electro-thermal de-icing systems. Flexible wrap-around heating mats can be installed directly onto the blade exterior with the use of adhesives as a retrofit application. Alternatively, the de-icing pads can be molded flush into the leading edge, with no aerodynamic losses. Rotorcraft de-icing systems are most likely constructed to employ composites rather than rubber boots due to high rotation speeds, which translate into higher loads per unit weight [7]. Electrical wiring for electro-thermal de-icing systems is not a significant design challenge within fixed wing aircraft as there is abundance of space inside the wing. However, the small blades of rotorcraft render wiring more difficult. More significantly the power distribution from a stationary airframe to a rotating rotor, creates a challenge. Due to sand and rain erosion problems, electro-thermal de-icing systems are also retrofitted with an erosion shield mounted onto the leading edge. This erosion shield will inherently serve another purpose by evening out the heat distribution and preventing cold spots [7]. Within a composite structure such as the one used for this system, it is important that the thermal expansion and contraction properties of all materials are relatively similar.

Tests have shown that most ice accretion occurs between 40-80% of the lifting surface's span, with the origin at the root. At the inboard portion of the blade the rate of droplet impingement is low and towards the tip kinetic effects and centrifugal forces are high, therefore in these regions, ice formation is at a relative minimum. This difference in the rate of ice impingement must be considered when identifying heater element location and power output.

A major design constraint is to minimize the electrical requirement of the overall system. For an efficient de-icing operation, a sufficient amount of heat energy must be efficiently supplied to the icing area. This constraint leads to the following design implications when designing an electro-thermal system [7]:

i. Applying heat to the entire blade is impractical - a power source larger than that available from the aircraft's power source is needed. Hence the heater mats are cyclically heated between blades, and further cycled between chord-wise or span-wise locations of the blade.

ii. Since atmospheric cloud ice forms only on the leading edge of lifting surfaces to 15% mean aerodynamic chord (MAC) on the top surface, and 25% MAC on the lower surface [5], heater mats are only needed in this region. However, if heat is applied only in this region, a possibility exists of the runback water refreezing further down the chord of the blade, possibly on critical components.

iii. The system can be made more efficient by applying high specific heat over a shorter time as opposed to low specific heat over a longer time span. The high specific heat input reduces the convection losses from the exposed ice surface, conductive losses to the structure and to a lesser degree, compensates for the uncertainty caused by the large variation in the bonding strength of ice.

iv. Good insulation between the heater and the supporting structure is necessary to ensure that all heat is directed towards the ice.

v. A chord-wise gradient to heat input may be required to encourage uniform melting of the bond over the protected surface. This will produce clean shedding, and help to avoid runback.

vi. Cycle off-time should be controlled to permit adequate ice accretion for the best shedding characteristics.

vii. Shedding symmetry: For a four bladed rotor, it is conventional to de-ice two opposing blades simultaneously. Unsymmetrical shedding will cause rotor unbalance, and potentially catastrophic vibrations.

Shedding zone power requirements are difficult to determine. Heat transfer rates, aerodynamic forces, and ice/substrate adhesive bonds are just some of the factors that affect the power requirements. Element-on-times (EOT) must be carefully chosen in order to effectively and uniformly melt the ice. Because helicopter rotor blades have comparatively small chord-lengths, EOT typically approaches 1 second at relatively warm temperatures, while fixed-wing aircraft use EOTs of much larger magnitudes [7].

As previously mentioned, in order to minimize power consumption at a given time and to increase efficiency, heater mats are arranged either span-wise or chord-wise on the airfoil. Typically, the heating elements are activated tip to root for the span-wise system, or stagnation point and outwards for the chord-wise systems. The design challenge of chord-wise sectioning is laying wire *within* the small rotor blade and would lead to a greater possibility of malfunction; however, this arrangement has proven to be more efficient [8]. Both arrangements are shown in Figure 4. Within the heating elements themselves power variations can be made by altering the resistance values or by varying the EOT to create a homogeneous ice melt distribution.

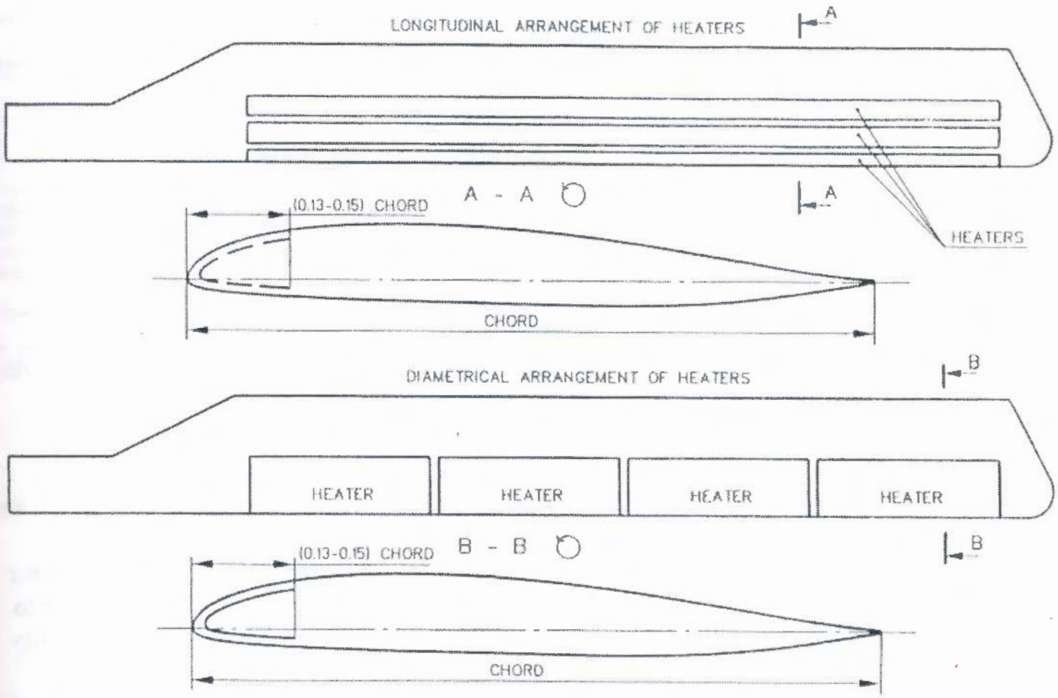

Figure 4. Span-wise and chord-wise heater cell installation layout.

The electrical system, which can either run on the existing helicopter electrical source or a separate dedicated system, must be properly sized for the required electrical load. This constraint often results in a larger power requirement than the existing electrical system can allocate. A second large electrical system needs to be installed due to FAA redundancy requirements in order to ensure safe operation when icing conditions are encountered. For a mid-size helicopter, the weight of an alternator alone is approximately 54 lbs. Due to this imposed restriction, major performance and cost penalties result [5].

In a pre-determined sequence and EOT set by the controller, a power pulse activates each element when triggered by a mechanical or solid-state switching device located in the rotor head. Power is distributed from the rotor mast to the rotating blades via a slip ring system.

The controller may be either an automatically or manually controlled system. In the case of an automatically controlled system, element on time is based on the ambient air temperature, or the icing rate, while the element off time is based on the icing rate. For manually controlled systems, the pilot can input the ambient air temperature, and use his/her judgment to determine the icing severity. Manually controlled systems are not recommended for composite blades however, since overheating problems are more of a concern.

Table 2. Weight breakdown of electro-thermal systems: [5]

Blade heaters (4 blades)	12 lb
Controls	12
Slipring and distributor	7
Wiring	13
Tail rotor system	10
Alternator and drive, No. 1	54
Alternator and drive, No. 2	54
Total	162 lb

Advantages	Disadvantages/Limitations
• Majority of aircraft certified to fly in icing conditions are fitted with electro-thermal systems, hence providing a large bank of knowledge in maintenance, repair, operation, and design • Effective and reliable • Action time virtually unlimited • Operating parameters are variable depending on atmospheric conditions	• Three major problems arise from this type of de-icing system: weight, electric power, and aerodynamic performance degradation • Power consumption is very large, and in some cases even impractical. Electrical de-icing systems for rotor blades use up to 12 kW of power to achieve all weather flight capability [1]. • Weight increases due to implementing electrical redundancy (2 alternators) according to FAA regulations (table 2). • Melt water runback. The fluid has a potential to refreeze in critical zones, degrading flight characteristics. Heating the entire blade to compensate for runback problems is extremely power consuming, and thus impractical

	• Element burnout. No redundancy exists, hence ice shedding may be asymmetrical which induces detrimental flight characteristics for rotor craft • Minimum ice thickness. Allowing the 0.3" ice build up induces moderate performance penalties. Tests on Bell 214ST, which has a 33" chord, 6-blade design experienced a 2.2% torque rise, and Bell 412, with a 17" chord, 4-blade design experienced a 10% torque rise [5] • ET systems give the highest cost per performance compared to any other de-icing system [5]

Table 3. Production helicopters certified for icing condition flight. [5]

Manufacturer	Aircraft	User	Gross Weight (lb)	System Weight (lb)	Type Heater	Electrical System	Heater Zones per Blade	Ice Shedding Sequence
Aerospatiale	SA-330	Commercial	16,300	200	Wire	AC	5	Chordwise
Bell	UH-1H	US Army	9,500	245	Foil	AC	6	Spanwise
Bell	412	Commercial	11,600	162	Foil	DC	4	Spanwise
Bell	214ST	Commercial	15,500	170	Foil	AC	6	Spanwise
Boeing Vertol	234	Commercial	48,510	N/A	Foil	AC	6	Chordwise
Hughes	AH-64	Commercial	13,800	103	Foil	DC	5	Chordwise
MBB	BO-105	Commercial	5,070	119	Foil	DC	6	Chordwise
Sikorsky	UH-60	US Army	20,250	N/A	Wire	AC	6	Chordwise
Westland	Wessex 5	Commercial	13,503	N/A	Spray-mat	AC	5	Chordwise

3.0 Pneumatic rotor de-icing

Pneumatic de-icing systems have been actively incorporated into fixed-wing aircraft designs since the 1930s. Their lightweight design, low power requirements and low initial costs have made pneumatic de-icing systems an excellent protection method for fixed-wing aircraft and, to a lesser degree, for rotorcraft as well. The concept once again is very simple: bleed air from the rotorcraft's engine compressors are fed through elastomeric tubes, prompting them to inflate. As the tubes inflate, the difference in the axial strains of the ice and elastomer destroys the adhesive shear strength of the ice/substrate interface bond, hence cracking the ice. Centrifugal and aerodynamic forces acting upon the shattered ice particles carry them away. If bleed air is not available from engine compressors, then a simple electrical dry pump is suitable [9].

The primary components of a pneumatic rotor blade de-icing system consist of a regulated pressure source, a vacuum source, and an air distribution system. Air filters, check and relief valves, control switches, timers, and electrical interfaces are also common components. A schematic pneumatic de-icing setup for rotorcraft application is depicted in Figure 5. A vacuum source is needed to ensure complete deflation of the tubes in order to maintain minimal aerodynamic penalties. Negative aerodynamic forces acting on the lifting surface can produce a low-pressure zone within the tubes, hence causing them to partially auto-inflate, providing a vacuum is not applied [10].

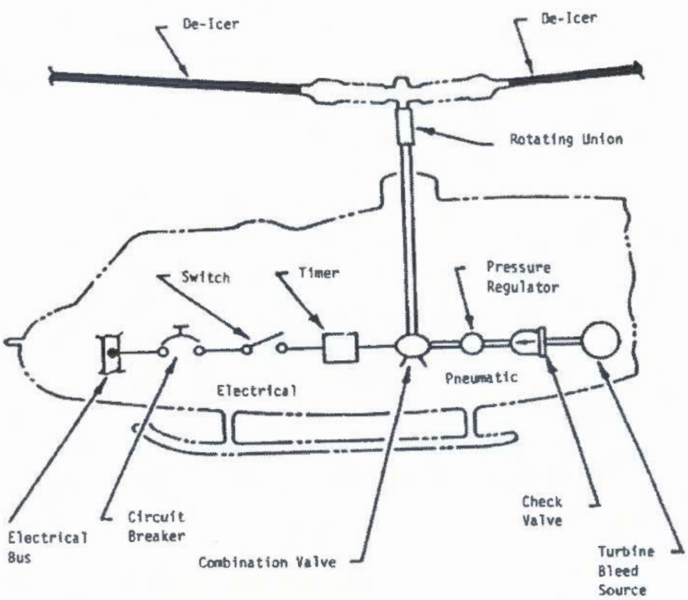

Figure 5. Pneumatic de-icing system schematic. [9]

The outer layer of the boot is a weather-resistant elastomer chosen for rain erosion resistance, and slow weathering properties. Directly below is a natural rubber layer, with its resilience to stretching helping to remove air once it is inflated. The weather resistant layer and the natural rubber are then bonded to a sheet of stretchable fabric to make up the upper layer of the de-icing blanket. The upper layer is stitched onto a non-stretchable fabric layer in such a way that air passages are created, allowing the stretchable fabric to form tube-like structures. The non-stretchable fabric is then bonded to another rubber elastomer layer, which acts as the bonding surface to the lifting surface. An autoclave cure is subsequently used to bond these materials into a relatively thick smooth blanket.

The de-icing boot is designed to inflate and deflate through a single air connection which is located on the installation side of the de-icing blanket. The blanket is mated directly over a supply hole protruding out of the wing's outer skin [9]. Roughly 1" of non-inflatable material may be used beyond the de-icing area to act as an edge seal in order to relieve installation stresses at the edges of the de-icing blanket [10]. Refer to Figure 6, for an illustration of a typical leading edge installation of a pneumatic de-icing system. When sewing the tubes, orientation – chord-wise or span-wise – plays an important factor. Span-wise tubes are more popular and de-ice with greater efficiency. However, chord-wise tubes produce much lower aerodynamic drag, and seen likely on airflow sensitive airfoils [1]. An example of span-wise and chord-wise tube orientation is shown in Figure 7a. Helicopter rotor blades have been tested with a de-icing boot, which incorporates span-wise tubes at the stagnation point, and then chord-wise tubes upon the upper and lower surfaces of the blade, see Figure 7b. During icing trials, the ice was effectively removed while also maintaining a minimal aerodynamic loss [ref 8 and 9].

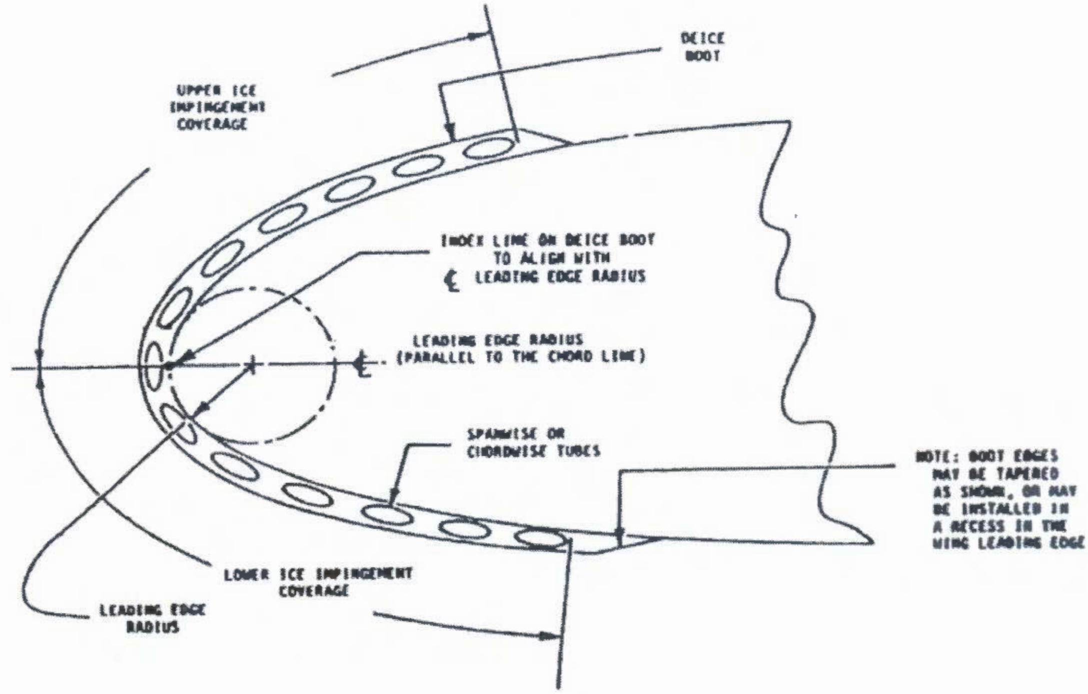

Figure 6. Pneumatic boot leading edge installation. [9]

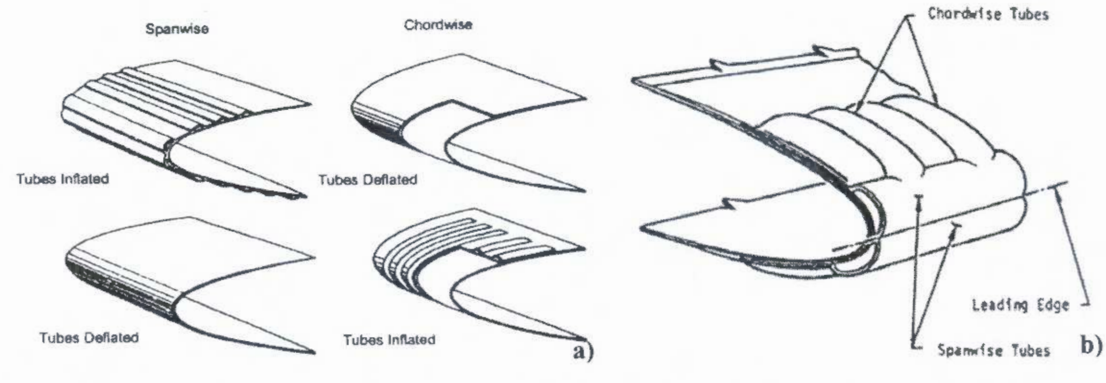

Figure 7. a) Span-wise and chord-wise boot orientations b) Proposed rotorcraft boot. [9]

Air from the engine's compressor is passed through several stages before entering the pneumatic tubes. The air is first fed through a check valve, and then through a pressure regulator. The check valve allows the system to be tested on the ground while the engine is not operating, and also allows single-engine operation for helicopters with more than one engine [10]. The pressure regulator reduces the bleed air pressure to that required for the de-icing system. Filters are also placed in the system to ensure that no debris will clog the pneumatic tubing. The vacuum is either obtained through a separate source or through an ejector flow valve solenoid, which will control both inflation and deflation. When a system timer energizes this valve solenoid, the ejector is shut off and the system pressure is directed to inflate the tubes. When the solenoid is de-energized, the air is expelled overboard, and the vacuum is reinstated. A rotating union is used to transfer bleed air from the rotor mast to the rotor hub where a connection is made to each blade [10]. A pressure switch may be placed in the air line to provide an electrical signal to the control panel, indicating successful tube inflation. Directly opposing blades or, ideally, all blades, should be inflated at the same time in order to ensure symmetric shedding.

Due to an interesting principle termed Elastomeric Self-Shedding, the pneumatic de-icer does not need to extend all the way to the tip. Due to the low modulus of elasticity of an elastomer such as rubber, it can deform relatively large amounts under shear loading. Upon rotor icing conditions, if a rigid sheet of ice was to form onto this rubber layer, the centrifugal forces (which are greatest at the tip) would axially strain the lower modulus rubber to a greater extent than the higher modulus stiff ice. This difference in axial strains would create stress concentrations at the surface of the rubber, and hence reduce the adhesive shear strength of the ice/substrate interface. The strain between the ice and rubber causes a shear stress at the interface, which will reduce the adhesive shear strength of the interface [10].

During the brief time of inflation, the deformed shape of the rotors will cause significant drag, resulting in a torque increase. This induced drag, however, is still not significantly more than the drag the pilot experiences at ice levels that pilots can tolerate [10]. Small roll, pitch, and yaw changes are detected, but are pilot-controllable [5].

Blade aerodynamics are essential since torque rises should be avoided in preventing deleterious vibrations, the blade can be recessed or contoured in order for the installed de-icing blanket shape to match that of the blade prior to boot installation. Alternatively, an autoclave cures the de-icer in a fiber-reinforced pre-preg material to form a leading edge shell, which can then be bonded to the blade in a replaceable assembly.

A pneumatic de-icing system was successfully tested on a Bell UH-1 helicopter (4310 kg or 9500 lb). Full span boots were simultaneously inflated in 2-5 seconds using compressor bleed air to effectively remove accreted ice. In another test, adequate results were obtained for test temperatures as low as -20°C, and LWC up to 0.8. The helicopter was tested in-flight at 91KCAS, a maximum torque-rise of 27% at maximum inflation was experienced, but for a very short time [5].

Generally, the pneumatic de-icing system in a rotorcraft is activated once the ice level reaches approximately 0.25" in thickness, either manually (visual reference point) or automatically (activated by an icing sensor). It should be noted that if the pneumatic de-icer is activated prematurely, a "bridging" effect may occur. Bridging is the formation of ice over the boot, which, if not removed during boot inflation, will intuitively cause detrimental aerodynamic effects. Boot inflation time is normally 2 seconds for rotorcraft applications [9].

An ice-phobic coating can be applied onto the boots prior to flights as well. This coating will help inhibit ice formation on the surface by reducing the adhesive strength normally attainable by the ice. Weathering problems, however, call for the need to re-apply the coatings after 50-150 flight hours.

The weight breakdown of two Bell helicopters, the UH-1H, and the Model 412 are outlined in Table 4; all weights are in pounds [5]:

Table 4. Weight breakdown of pneumatic de-icing systems.

Component	UH-1H (Ref.5)	Model 412
Blade boots	21	34
Components	4	5
Plumbing	15	15
Total	40	54

Power required for each inflation cycle was determined to be 370 watts, producing an air volume flow rate of 22ft^3 per minute. In summary, some characteristics of a conventional pneumatic boot system are listed below:

- Surface ply elongation 40% to 50%
- Nominal inflation time 2-5 seconds
- Nominal deflation time 6 seconds
- Maximum surface distortion 9.53 mm (0.375 in.)
- Threshold ice removal thickness 6.35 mm (0.25 in.)
- Surface ply material Elastomeric

Advantages	Disadvantages/Limitations
• Minimal mechanical parts, little servicing required • Repair, maintenance, inspection, and replacement concerns are well understood due to years of experience • Light weight, low cost, and low power requirements • Proven and reliable (on fixed wing)	• An aerodynamic penalty (torque rise) is associated with boot inflation, especially in rotor blades as lifting-surface is small • "Bridging" effect of ice if system is activated prematurely • Rain erosion resistance studies need to be done for an adequate elastomer. Elastomer lacks durability and adequate rain erosion properties • Poor efficiency at low temperatures • Possibility of considerable outer surface deformations even when de-icing is not on • High complexity of transmission of compressed air from a non-rotating element to a rotating rotor • Impossibility of combining pneumatic de-icing with leading edge erosion protection

Small tube pneumatics (STP)

During the 1920s, as a side product of ice-phobic coatings research conducted by B.F. Goodrich, the concept of small tube pneumatics was developed. The concept is identical to normal pneumatic de-icing, except that small flat tubes, high pressure, and short intervals are used to de-bond thin layers of ice. STP can de-bond ice thickness' of 2.5mm (0.1") as compared to 6.4mm to 12.7mm (0.25" to 0.50"), which are achievable by conventional pneumatic systems. Boot tubes are inflated using 862 kPa pressure compared to 124-172 kPa pressure in standard pneumatic devices. STP was developed as a means to remove thinner ice formations and smaller ice particles than conventional pneumatic devices [11]. Recent testing (part of the USAF/NASA "low power" de-icing system evaluation) of a STP de-icing system at NASA's Lewis Icing Research Tunnel was conducted on a 533mm chord NACA 0012 airfoil representing a helicopter main rotor blade. The test de-icer was 1.9mm think, with a weight of 2.4kg/m^2. Testing resulted in residual ice of 2.5mm thick remaining for icing intervals up to 20 minutes.

4.0 Pneumatic Impulse Ice Protection (PIIP)

B.F. Goodrich [11] developed an advanced de-icing system called Pneumatic Impulse Ice Protection with goals of achieving:

a) Reduced minimum ice thickness prior to efficient application

b) Reduced particle shedding size

c) Enhanced weatherability of surface erosion material

De-bonding of ice is accomplished by introducing a stream of controlled high-pressure air through span-wise tubes. As the expanding air traverses outwards, the surface is forced to snap outwards rapidly, thereby inducing bending stresses within the ice/substrate interface, and resulting in ice fracture. Due to the high stiffness of the surface, the leading edge will return to original shape with a high normal velocity, hence also assisting in rapid air removal. The expanded air is then vented via ports located in the backside of the de-icing tube. A basic schematic model of the operation principle of the pneumatic impulse ice protection system is shown in Figure 8.

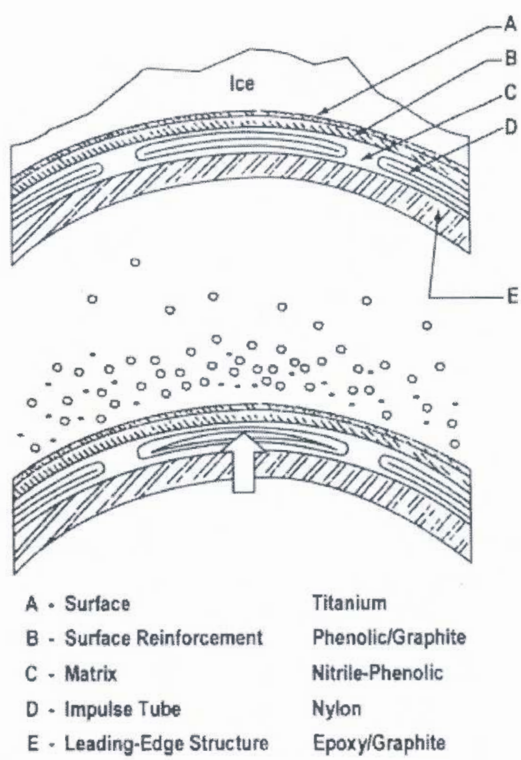

Figure 8. PIIP schematic. [12]

A weather-resistant erosion layer, usually a titanium sheet, a high-performance thermoplastic called polyetherketone (PEEK), or a toughened, impact-resistant, fabric reinforced thermoset resin, is used for the surface material of the system, which then overlays onto a quasi-flexible polymer matrix. Span-wise fabric reinforced tubes are located within this matrix [12]. The location of these tubes, with respect to the blade geometry, is determined by analysis and testing of ice droplet impingement studies.

Impulse valves regulate a precise quantity of high-pressure air entering the impulse tubes. Once these valves are activated by a signal from the controller, supply air to the valve from the reservoir is shut off, allowing impulse air to expand through the de-icing tubes. During de-activation, the air supply to the valve is re-charged completely, usually within one second. The quantity of air supplied to the impulse tubes is typically sufficient to de-ice 8 ft^2 of surface area, hence each blade has small sections for de-icing. Activation timing of the system, usually 0.05 sec, is determined by the controller [12]. The controller, at repeated and fixed time intervals, sequentially and symmetrically actuates the valves in order to maintain symmetric shedding. Either the pilot, or remote sensing devices, control initiation. System operating pressure is 4140 kPa (600psig) for PEEK, and 8280 kPa (1200 psig) for the titanium surface material [12]. The high-pressure air is either supplied by a motor (electric or hydraulic), a stored air reservoir, or another high-pressure pneumatic system.

The impulse valves are preferably located as close as possible to the de-icing area in order to minimize diminishing impulse strength. Typically, the valves are located directly behind the leading edge surface, connected directly to the de-icing tubes. However, in rotorcraft, internal access is not practical. In this application, the valves are either located externally or somewhat remotely distanced from the inlet port, resulting in decreased surface area that can be effectively de-iced. For rotary wing applications, 2 impulse valves are needed (1 for each side of the stagnation line), positioned near the root of the blade. Each impulse valve contains an internal chamber to accumulate air of predetermined volume (~0.025 m^3) [11].

Depending on the application or aerodynamic sensitivity, the de-icing system can be installed in a number of ways [12]:

- Skin bonded – a de-icing blanket is bonded to the leading edge similar to the method of conventional pneumatic de-icing systems. While resulting in aerodynamically intrusive properties, it can be retrofitted to most applications and facilitates easy removal and replacement.

- Recess bonded – Basically the same principle as the skin-bonded method, however the outer surface of the airfoil is recessed, resulting in no aerodynamic losses.
- Integrated Composite Leading Edge Assembly - The de-icing blanket is co-cured onto a composite rotor structure to form a stand-alone composite leading edge assembly with a built in de-icing sytesm. This is the most desirable method for an aerodynamically non-intrusive installation.
- Modular Composite Leading Edge Assembly – The surface assembly of the de-icing system is mechanically attached rather than resin-bonded to the underlying portions of the system and leading edge structure. This arrangement allows the surface assembly to be removed and replaced as a separate item should the surface be damaged, without requiring replacement of the entire leading edge.

Table 5. Weight, power, and size specifications of a PIIP system. [12]

Item	Unit Weight	Quantity or Application	Power	Envelope Dimensions
Deicer	0.50 lb/sq.ft.*	-	-	0.100" thick
Impulse Valve	1.0 lb.	1 valve/8 sq. ft.	300W***	5.5" x 4.2 x 1.5"
Compressor	21.0 lb.	one	1.6 gpm**	11.5" x 9 x 10.3"
Controller	1.0 lb.	one	3W	4.8x 4.0 x 3.6"
Regulator	0.2 lb.	one	-	2.6" x 2.0 x 1.0"
Shut-Off Valve	0.8 lb.	One	24W	3.2" x 2.5 x 2.0"
Pressure Switch	0.2 lb.	One per impulse valve	-	2.5" x 1.0 x 1.0"

Advantages	Disadvantages/Limitations
• Low power requirements • Aerodynamically non-intrusive design achievable • Thin ice removal capability: 0.08" to 0.1" ice thickness in all icing conditions, and ice shed particle sizes less than 0.25" equivalent spherical diameter • No minimum or maximum ice thickness required or recommended for efficient system operation • No runback and re-freezing	• Field knowledge limited since no aircraft currently certified with PIIP • Noise associated with pulsing • Fatigue of de-icing system is a concern, limited data since lack of operational experience • Transmission of high pressure air through a rotating union is difficult

5.0 Fluid Anti-icing

The concept of anti-icing with a fluid is very simple. Basically, the fluid, which is a Freezing Point Depressant (FPD), comes into contact with super cooled water droplets and considerably lowers the freezing temperature of the water. The fluid mixture flows along the airfoil by the influence of the boundary layer, and either evaporates or is shed from the trailing edge. The two primary means of distributing this liquid onto the airfoil is via porous leading edge panels or through spray nozzles.

Icing control using fluids can be categorized into 3 classes: anti-icing, natural de-icing, and de-icing. Typically, most fluid systems are anti-icing systems, whereby a sufficient amount of fluid is present to lower the freezing point of water. Anti-icing systems are generally applicable for light to moderate icing conditions. When the icing condition becomes more intense, ice will likely form on the point of maximum impact of water droplets, which is usually at or near the stagnation point. The fluid pump rate is usually too low to prevent ice accumulation at these conditions, letting the ice accumulate. However, with the combination of centrifugal and aerodynamic forces, and the effect of the FPD fluid on the substrate/ice bond, the ice will not be able to fully bond to the surface and will be carried away. This type of icing control is called natural de-icing, which is very similar to normal de-icing, the only difference being that ice will be allowed to accumulate to a predetermined thickness before the icing system is activated. Fluid de-icing is not recommended, since evidence exists to suggest that this method may not be reliably effective [13].

The first application of fluid anti-icing systems was implemented in the 1930s onto fixed winged aircraft by the British company, Kilfrost, in a very simple design consisting of fabric wicks covered with wire gauze. As the need for a more effective and reliable systems grew, the British government formed a new company, TKS, by bringing together three different leading companies with the appropriate specializations. In the 1950s, TKS produced a revolutionary system, which efficiently pumped and distributed the FDP fluid through, initially, a porous powder stainless steel leading edge panel and, with more development, later through a rolled and sintered wire cloth. The porous panels constructed of the sintered wire cloth, proved to be a very effective method and is still a focus of significant production [13]. Testing has recently been conducted on Bell UH-1 helicopters incorporated with a fluid anti-icing system (glycol/alcohol solution) and acceptable results were obtained. Tests that were conducted at temperatures as low as -20°C, with liquid water content of 0.8, 0.9 lbm/min fluid flow rate, revealed adequate measures to prevent ice formation. With this flow rate, however, protection of only up to 1 h. 24min could be obtained. Bell concluded that fluid anti-icing was the best system for the UH-1 but at the time there was no funding for additional development [5].

There are several chemicals that when mixed with water, will lower the freezing point of water. Glycol, alcohol, calcium chloride, nitric acid, and sodium chloride are examples of these chemicals. Monoetheylene glycol (MEG) is the most widely used chemical utilized in FPDs in the aerospace industry. The viscosity of MEG is within adequate limits, as well as its volatility (it is a negligible fire hazard) – all of which are problems associated with alcoholic solutions. The two most commonly used solutions are TKS 80, and DTD 406B (also known as AL-5). Anti-icing fluid characteristics are presented in Figure 9a and Figure 9b.

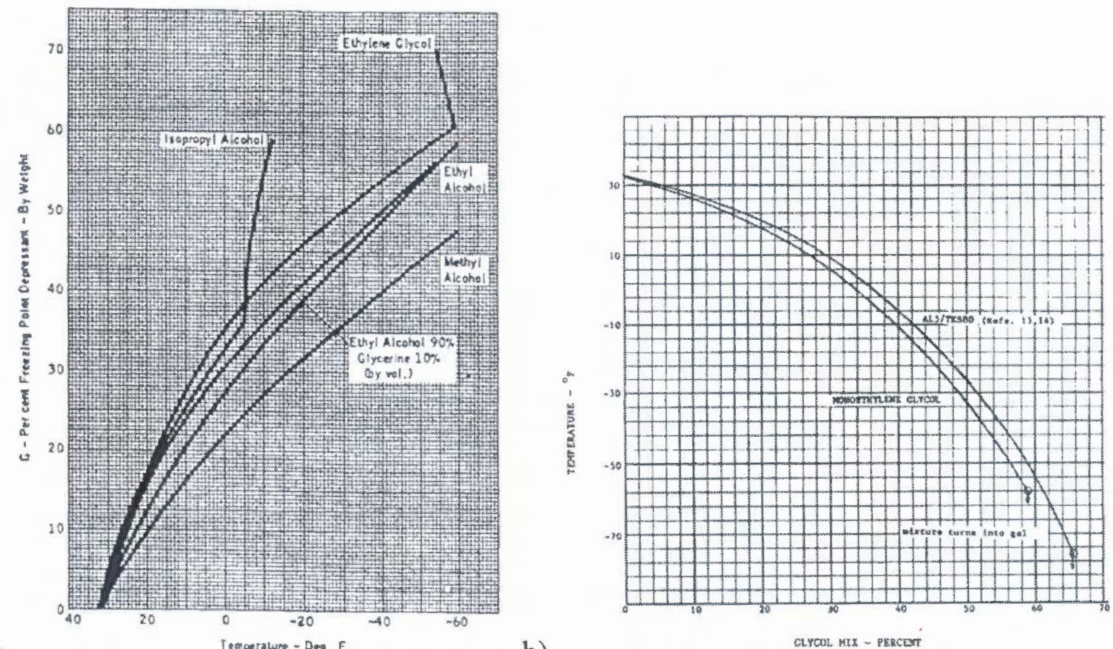

a) b)

Figure 9. Characteristic curves for common ice phobic fluids: Freezing temperature vs. percent weight FPD. [13]

The FPD is stored in a convenient location in the aircraft where it can be readily filled or repaired. Nylon tubing, ranging from between 0.5cm to 1.27cm outer diameter is used to distribute the fluid to system components [13]. The pump, usually driven by a DC motor, produces relatively constant flow rates at all times. The pump can have pre-set flow rates for specific conditions, but usually manual flow rates are controlled by the pilots. For automatic actuation, an ice sensor would be placed upon the blade, and would signal the controller for operation of the system. Depending on the icing rate measured, the ice sensor could also be used to determine a flow rate. For manual actuation, the pilot would have to rely on a visible object: this could be difficult for main rotor blade de-icing. A schematic of fluid anti-icing systems is shown below.

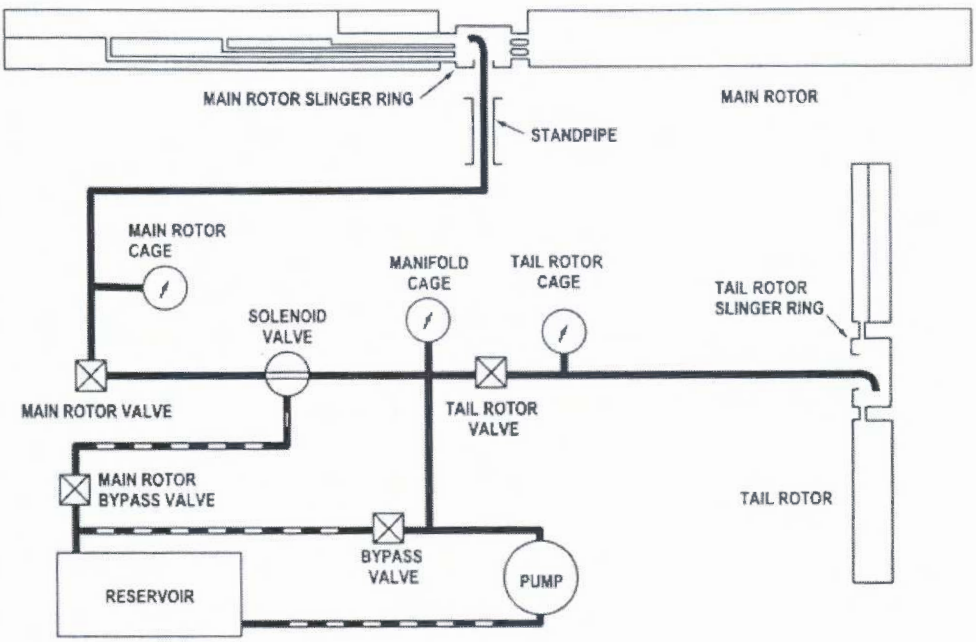

Figure 10. Schematic setup for a rotorcraft fluid ice protection system. [13]

The porous panel (Figure 11a) of several layers (depending on strength requirements) is typically constructed from sintered and rolled stainless steel mesh, or laser-drilled titanium for the outer skin. A stainless steel or titanium back plate is used to form a reservoir. To maintain sufficient resistance to fluid flow, in order to retain adequate reservoir pressure, a porous plastic liner is added, (Figure 11b). The use of titanium, as opposed to steel, reduces the weight by 50% while providing greater resistance to impact damage, and improved surface finish [13].

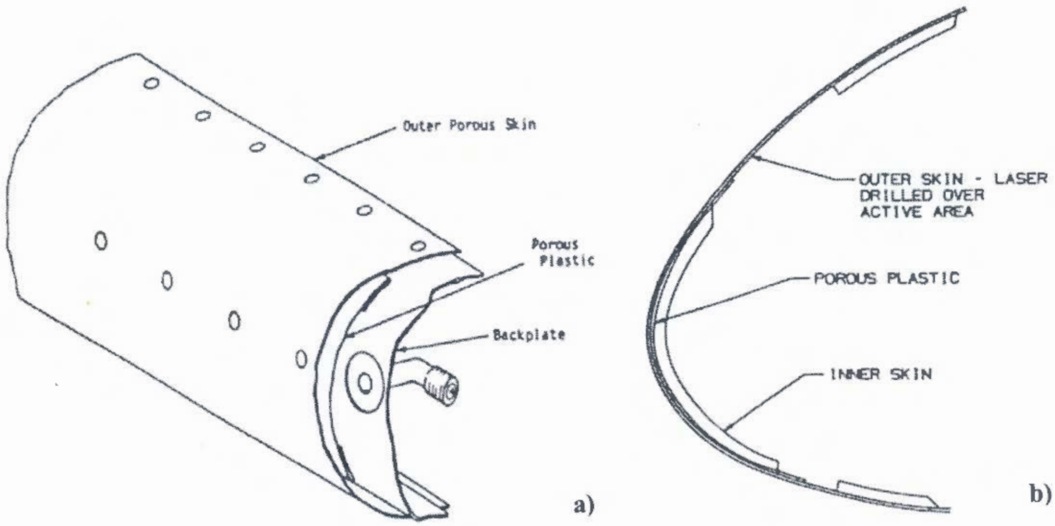

Figure 11. a)A typical view of a porous panel b) Cross section of a porous panel. [13]

A slinger ring is used in the de-icing system to distribute the fluid from the fixed frame to the rotating rotors. Flexible hoses are used to supply the fluid from the slinger ring to each blade. The OEM helicopter blades would be retrofitted with forward and aft grooves milled into the nose block of the airfoil as channels for fluid flow, and holes drilled into the leading edges (see Figure 12). The anti-icing fluid channels down the aft groove, then forward to the two leading edge grooves, and escapes through the porous leading edge panel. If holes are drilled into the leading edge and abrasion shield rather than using porous panel, then intuitively optimal blade diameter and positions need to be determined for uniform surface wash. Experiments have shown that in order to have most uniform distribution, the blade is divided span wise into sections and liquid is delivered to each section uniformly [3].

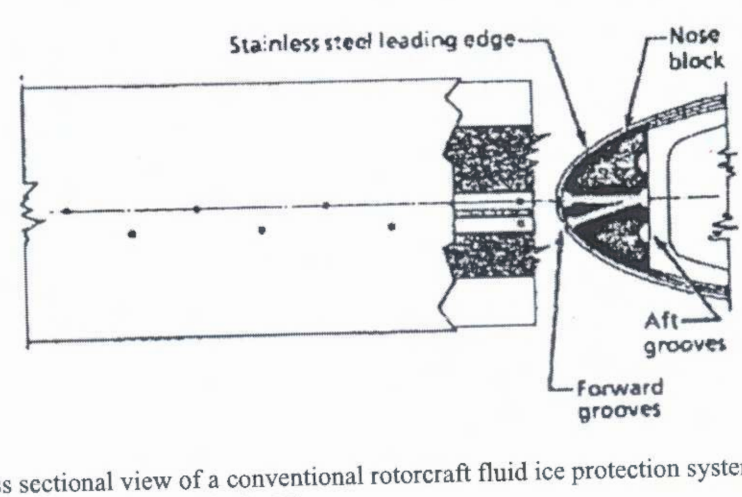

Figure 12. A cross sectional view of a conventional rotorcraft fluid ice protection system. Note the forward and aft grooves milled into the nose block. [5]

Operating weight is a limiting factor of fluid anti- and de-icing systems. An outline of the weight breakdown for a typical rotorcraft (Bell 412) fluid ice protection system [5] can be seen in Tables 6 and 7. At 117 lbs, the weight of the fluid alone would result in a weight larger than most other de-icing systems, while only providing de-icing capability for a duration of 1 hour.

Table 6. Fluid weight calculation

Alcohol/Glycerin	6.92 lb/gal
Specific flow rate	0.015 qt/min/ft
Length of protected leading edge	18.8 ft
Number of blades	4
Flow rate	1.95 lb/min
Fluid required	117 lb

Table 7. Anti-icing system weight breakdown

Blades	28
Pump and tank	13
Main rotor slinger ring	7
Tail rotor slinger ring	2
Controls and panel	15
Link and fittings	5
Trapped fluid	7
Empty weight	77
Fluid (1-hr duration)	117
Total	194 lb

While MEG is toxic, it provides no danger to humans unless ingested in large amounts. It is estimated that the lethal ingestion dosage for humans is 100ml. The threshold limit to cause any major health side effects is approximately 125mg/m^3 [13], which is far beyond the vapor concentration produced by MEG under normal conditions. With respect to the environment, experiments have shown that MEG is biodegradable, and will completely break down in 3 days at 20°C [13].

Advantages	Disadvantages/Limitations
• Anti-icing system rather than de-icing system: there is no ice accumulation at any point, hence no aerodynamic penalties result • Porous leading edge panels, flush with airfoil. No aerodynamic penalties • Melt water runback refreezing is prevented due to runback of anti-icing fluid, therefore no freezing in critical areas • Low power consumption required,	• Finite period of protection, dependant upon fluid supply • Initial cost higher than pneumatic system • Fluid weight reduces useful aircraft load • Added maintenance needed: Fluid must be refilled • Fluid may not be available at every airport, hence extra supply should be carried on-board, further increasing the

typically only 30-100 watts • Hardware weight is comparable to or less than other systems • All components, aside from the fluid and filters, are designed for the life of the aircraft, resulting in low maintenance costs • Pilot skill and judgment to operate the system are minimal • The system can be used to remove leading edge contamination (insects, etc.) • The rotating action by the rotor causes the system to act as a large centrifugal pump, hence helping to minimize the pump size needed, and lowering costs • Mechanically reliable. Pump is the only moving part	weight • Fluid anti-icing does not guarantee ice removal once ice formation has already commenced • No icing protection at very low temperatures (MEG's freezing point is -22 to -40°C, depending on concentration). Icing encounters to temperatures as low as -40°C

6.0 Electro-vibratory De-icing

Basically, the electro-vibratory system de-ices by shaking the rotor blade at its major natural frequency. The resonant frequency at the interface and g-forces created by the amplitude of the vibrations create shear forces at the ice-substrate interface. A combination of the shear forces and friction generated by vibration of the blade's aluminum and ice particles will together melt, and ultimately de-bond the ice [1].

Extensive work has not been conducted on electro-vibratory de-icing concepts. One feasible study, which included laboratory testing, conducted by Bell Helicopter [5] under U.S. army sponsorship, is a noteworthy exception. In this study, a number of electric motor-driven configurations were investigated (see Figure 13). The shaker, which consists of 1.25 lb eccentric weights driven by a 0.5hp motor, was mounted onto the spar of a Bell UH-1D blade[1]. A water spray rig was used to coat a stationary blade at temperatures ranging between -5 and -15°C. It was determined that frequencies ranging between 0 and 47Hz with 25-35 gs, for a time span of 2 seconds would de-ice the blade satisfactorily except for the blade tip. It was also estimated that such a system for a Bell UH-1D helicopter would require approximately 1.3kW of electrical power, and have a gross system weight of 67lb. Fatigue loads experienced by the aluminum blade were marginally acceptable. However, for composite blades this would be less of a problem.

[1] 21 inch chord, 48 ft diameter

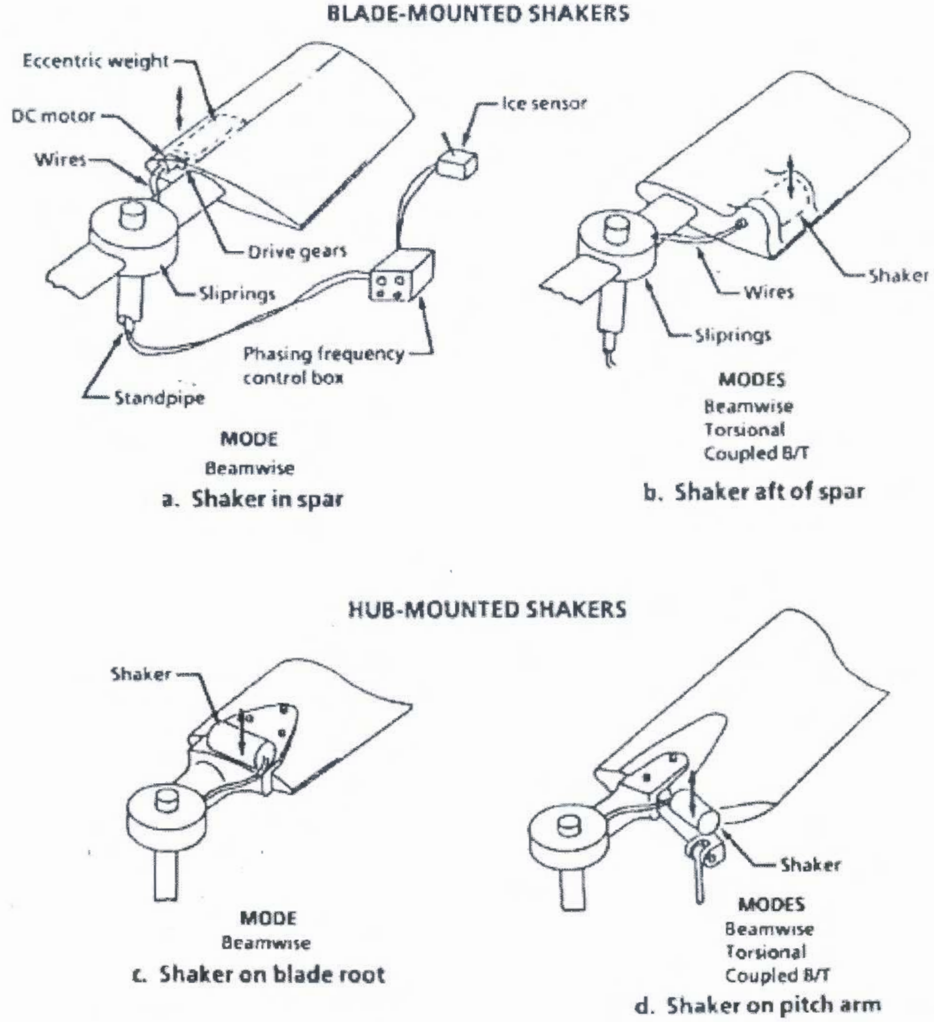

Figure 13. Possible mounting positions of blade-mounted shakers. [5]

Advantages	Disadvantages/Limitations
• Significantly lower power and relatively lower weight than electro-thermal • Complexity of installation similar to any other type of electrical de-icing mechanism	• The blade could not be de-iced well at the tip. Possible solutions include a thermal mat, Elastomeric self-shedding (see Pneumatic Rotor De-icing), or reliance on kinetic heating • Fatigue problems can be associated with electro-vibratory de-icing systems • Vibrations may cause adverse effects on aerodynamic properties and structural integrity of blades and frame

7.0 Electro-Impulse De-icing Systems (EIDI)

In order to de-bond and shatter accumulated ice, electro-impulse de-icing systems use electrical discharges to create large magnetic repulsive forces. Rapid normal accelerations are induced on the wing or blade's skin and are able to remove very thin layers of ice and produce very small particles. These systems have been known to use less than 1 percent of the energy of electro thermal systems of similar capacity.

Copper or unalloyed aluminum ribbon wire coils, typically 50mm in diameter and 3-5mm in thickness, are rigidly mounted underneath the surface to be de-iced. A small air gap separates the coils and the aircraft skin. High energy capacitors, which connect to these coils, discharge high voltage typically 800-1400V of electrical current [14]. The directionally changing current within the coil induces a rapidly forming and collapsing electromagnetic field which in turn produces eddy currents within the leading edge (Figure 14). The circuit must have low resistance and inductance to permit rapid discharges (typically a fraction of a millisecond). The opposing direction of eddy currents in the skin and discharged current in the coil will create repulsive electromagnetic fields, generating a peak force of 400-500 lbs to the skin [14]. The actual surface deflection is small, generally less than 0.25mm (0.01in), but the normal acceleration is rapid. A cross-sectional schematic of the impulse coils mounted onto the skin of a wing is shown in Figure 15.

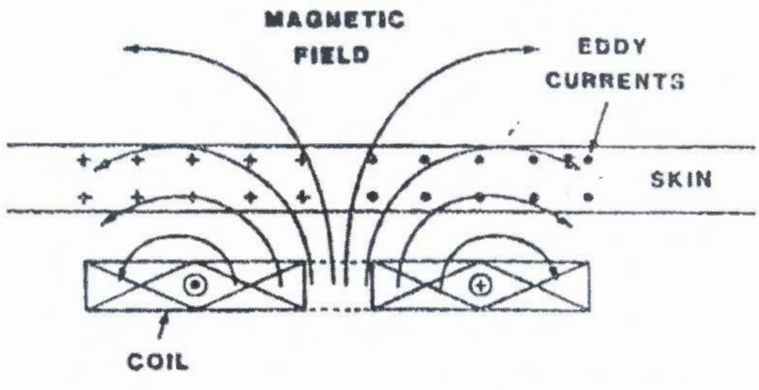

Figure 14. Coil magnetic fields and resulting eddy currents produced in skin due to coil discharge. [15]

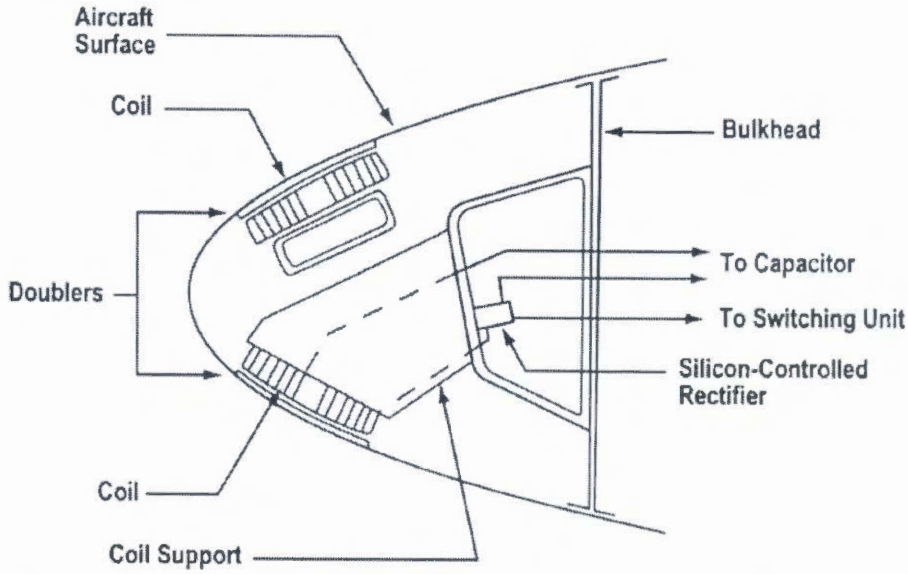

Figure 15. Electro-impulse coils mounted on either airfoil skin or internal supporting structure. [14]

The coils are typically mounted to the wing spar, or a beam between ribs, or directly to the surface to be de-iced. Regardless of the mounting position, the coil mount itself should be fabricated from a composite material. Typically, several layers of fiberglass or a composite sandwich are used to avoid electrical interaction with the coil's magnetic field. Coil mounts must also be rigid to avoid energy losses in the form of mount flexing. The air gap, which exists between the coil and the de-icing surface, must be large enough to compensate for the normal acceleration of the skin. Mounting the coils onto the skin would result in greater efficiency, as the skin would absorb all mechanical energy. Weight, performance and the aircraft's other primary structures would not be affected. However, designing a system that is mounted directly onto the skin requires much detail and care [15].

Coil placement is another critical issue, as the damping effect of the rotor substructure calls for the need to have the coils placed closer together than what is needed for typical hollow wing structures. Due to the high ampere per turn characteristic of the coils, the impact zone will be relatively small, and impact stresses near the edge of the coil may be close to zero [15]. A structural dynamic analysis, therefore, would be needed to determine coil placement for maximum de-icing efficiency. For fixed-wing applications, the spacing between coils is nominally 0.5m (18 inches), but largely depends on wing structure.

The airfoil shape and structure is also a concern. Blades with radii of greater than 25mm would be relatively easy to de-ice. Blades, however, with a flat upper and lower shape characteristic and a radii of less than 10 mm, would be difficult to de-ice. If the rib flanges, are riveted or bonded to the leading edges, then EIDI motion is hampered due to rigidity and therefore hollow structures are most suitable [15].

If the skin conductivity is insufficient, then doublers are mounted on the skin structure, within a polymer boot [5]. Doublers are usually copper or unalloyed aluminum disks that have a higher conductivity than the de-icing surface. These disks are slightly larger than the coils themselves, and even though they would stiffen the skin, the doublers would act to distribute the impulse load more evenly.

Each coil receives 2 to 3 electrical pulses from the capacitor with sufficient time (approximately 2 to 4 seconds) necessary to recharge [14]. The capacitor is then switched to the next coil, and ultimately cycles around the full aircraft. An example of an EIDI set-up upon a fixed wing aircraft, and indicating how switching between coils would be carried out is shown in Figure 16. The capacitor is discharged when a solid-state switch is triggered close to the circuit. This high-voltage, rapid response switch is a silicon-controlled rectifier, or "thyristor". Basic EIDI circuits (see Figure 17), aside from the switch, capacitor and coils, would include a power- and coil-sequencing switch box. A clamping diode is also used to prevent reverse charging of the capacitors. The capacitors receive their energy from a low voltage power converter that runs off of the aircraft's standard power supply [11].

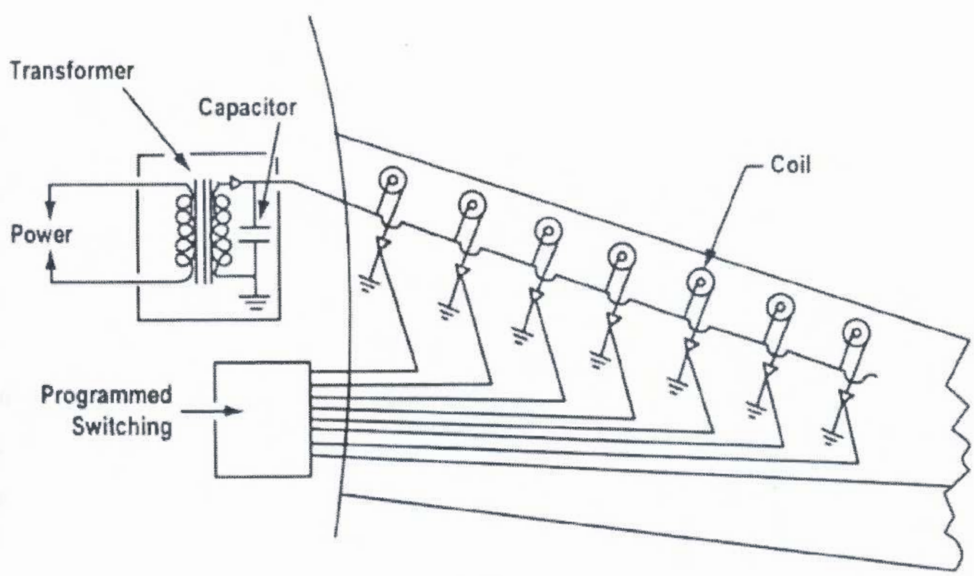

Figure 16. An EIDI system for a fixed wing aircraft. [14]

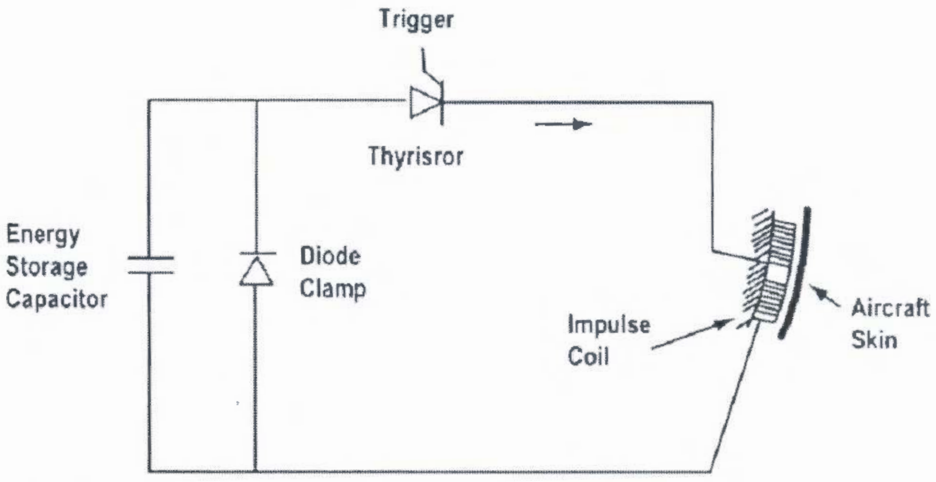

Figure 17. A basic EIDI circuit. [14]

Installation of the capacitors should be located close to the coils to reduce power dissipated by the high voltage current traveling down the lines. A trade-off study would be necessary to establish the numbers of coils per capacitor. Increasing the number of capacitors would minimize the dielectric losses in the lines. However, this would serve to increase the cost and weight of the overall system. Using more than one power box supplying energy to the coils would ensure that power would be distributed to the coils in the event of a power box failure. Alternatively, even and odd-numbered coils could be cross-connected to separate power boxes to limit ice accretion in the event of a power box failure. Power and sequencing boxes are normally located in the rotating hub, with a commutator ring bringing the low voltage current to a transformer. A rectifier is also placed in the hub to continuously recharge the capacitors [14].

EIDI systems have undergone extensive testing in NASA's Lewis Icing Research Wind Tunnel. Actual in-flight testing has been conducted by NASA, Cessna Aircraft Company, Boeing (757, leading slat 767) [14,5]. Various institutions have conducted other wind tunnel and electromagnetic tests. Unfortunately, the EIDI systems for rotorcrafts have not proceeded past the development stage. Retrofit applications are not possible since the coils and wiring cannot be placed easily onto an existing blade. If an EIDI system is to be used, it should be designed into the blade during development of the aircraft due to balance and aero-elasticity concerns. One possible mounting method for EIDI equipment is to recess the coils in the leading edge, and therefore a metallic leading edge and abrasion shield, would then be placed on top. If the abrasion shield has insufficient conductivity, then doublers can be used.

The weight and power requirements for EIDI systems of 3 different classes of aircraft are shown in Table 8. A basic extrapolation of EIDI system power of fixed-wing aircraft can be performed to estimate the EIDI weight for a helicopter such as the Bell 412. The 412 has a maximum take off weight of 11,900 lbs. Using extrapolation based on the weights of both a 6-passenger and a 150 passenger aircraft, an estimate of the weight of an EIDI system for the 412 can be determined. A typical 6-seat propeller driven aircraft has an approximate weight of 3,500 lbs, and a 150-passenger transport has an approximate weight of 120,000 lbs. Therefore, by extrapolation based on the weights of the aircraft and their corresponding EIDI system weights from Table 8, the weight of an EIDI system for the helicopter can be roughly estimated to be 80-100 lbs.

Table 8. Weight and power requirements of EIDI systems.

Aircraft	Power*	Weight**
6-place, propeller driven	400 watts	60 lbs***
150 passenger turbofan transport		
no redundancy	2 kilowatts	250 lbs
full redundancy	2 kilowatts	400 lbs
250 passenger transport		
no redundancy	3 kilowatts	350 lbs
full redundancy	3 kilowatts	500 lbs

Advantages	Disadvantages/Limitations
• Low power requirements: power usage is less than 1 percent of electro thermal or hot air de-icing systems of the same capacity. Power requirements are equivalent to landing lights for the same aircraft, hence able to run off standard aircraft power supply. For a medium size helicopter (10000-15000 lb) 3kW is typical [5] • Reliable de-icing: Ice thickness ranging from 8 to 26mm (0.03 to 1.0 inch) have been consistently removed, leaving only residual traces. All types of ice are effectively removed • Electromagnetic interference – Laboratory testing has failed to detect appreciable interference • No aerodynamic penalties • Weight comparable to other electrical based de-icing systems (~120lb) [5] • Low maintenance: No moving parts • No run-back re-freezing problems • No threshold ice thickness necessary for system operation, therefore no torque, aerodynamic penalties, and minimal pilot skill	• Design and operational experience limited • A de-icing system, not anti-icing • Complex design requirements • Loud discharging • Possible fatigue of skin, coil mounts – laboratory testing upon small aircraft. Aluminum and composite leading edges however have shown no fatigue damage after number of applied impulses equaling expected discharges in a 20-year lifespan • Lightning strikes – since EIDI is electrical, possibility of system being disabled, or other adverse effects. A system overload electrical components are needed

8.0 Coatings

Ice-phobic coatings have shown an ability to decrease the adhesion strength of ice under certain LWC and temperature regimes, but do not have the capability to perform sufficiently over the entire FAA icing envelope [16]. Surface treatments suffer from rain erosion and short life span of the applied chemical. What is needed is a durable and weatherable ice-phobic surface material that prevents ice from accreting in the absence of applied heat, power, or chemicals.

In the following text, only two separate topics will be discussed due to the large nature of the subject. The first topic will discuss research conducted by Dr. Terry Foster, entitled "Investigation of Novel Ice Release Coatings" [17], whereby ice bodies on a variety of different coatings were subjected to different mechanical tests. The second section will describe a unique electrically-based coating which was developed by Victor F. Petrenko, and Zoe Courville of Dartmouth College [18].

8.1 Investigation of Novel Ice Release Coatings

Dr. Terry Foster performed in-depth tests, such as torque/shear, impact, tensile, ice accretion, and weather susceptibility testing on de-icing capabilities of various coatings. Brass or aluminum rods abraded with 320 grit paper were coated and centred in brass cylindrical wells. Fifteen ml of water were injected and frozen at a predetermined temperature and time. A snap-on torque meter was used to measure the torque adhesion value of various test samples. Torque tests were conducted with and without coatings, for various types of frozen water. Large quantities of tests were performed, with conditions between tests varying considerably. A fair comparison of these different results is therefore questionable.

In the uncoated condition, average shear stress recorded by boiled distilled water at a –10°C freezing temperature recorded the highest value compared to any other type of water. Average shear stress was seen to diminish for decreasing temperature and increasing freezing time. Natural seawater exhibited much lower shear stress values compared to distilled water, with a magnitude of 3 to 4 times lower.

Torque adhesion tests were then performed on the same bars, with an alkyd coating at -20°C for various types of frozen water. Once again, boiled distilled water exhibited the highest values with natural sea water scoring considerably lower values. Trends also showed that with an increasing freeze time, the average shear stress decreased for distilled water. The opposite effect was shown in natural seawater. The effect of the coating was clearly pronounced for natural and synthetic seawater, the adhesion strength reduced by a factor of over 50% (1055 kPa and 483 kPa to 449.5 to 216.4 kPa, respectively). Torque testing was also performed under the same conditions as above on various other coatings, some with additives. Results indicated a significant number of coatings that exhibited even a *lower* torque adhesive strength than that of the alkyd coating. Some of these coatings demonstrated unacceptable weathering and erosion problems.

Tensile shear adhesion tests were also performed using the same setup as the torque shear adhesion tests, differing only in that the bars were not twisted, but pulled via an Instron tensile tester. Water was frozen for 3 days at approximately –22°C. Results showed that the average TSS was 1450 kPa, however no results were shown with a coating layer.

As a result of the tests for evaluated permanent coatings, it was determined that Alefro FX and Alefro SIII had the best combination of ice release, re-coatability and weathering properties. Of temporary coatings, even if they exhibited sufficient performance, they would not have adequate integrity to withstand more than one de-icing cycle, and were possibly even weak enough to be removed by water.

Advantage	Disadvantage/Limitations
• Low maintenance, as not a mechanical system • Anti-icing rather than de-icing • No pilot skill required	• Very poor durability and weatherability problems: continuously re-applied • Not reliable • Some coatings may not cover whole icing spectrum

Dr. Foster's test data is shown in the subsequent tables:

Table 9. Shear adhesion of various types of ice to uncoated brass rods. [17]

SHEAR ADHESION OF VARIOUS TYPES OF ICE TO UNCOATED BRASS RODS				
WATER USED/ TEMPERATURE (°C)	FREEZING TIME (hr)	AVERAGE SHEAR STRESS (kPa)	STANDARD DEV. (kPa)	NUMBER OF READINGS
BOILED, DISTILLED, -10	16/25	1890	437	20
BOILED, DISTILLED, -20	1.25/5	1603	397	25
BOILED, DISTILLED, -20	16	1542	414	15
SYNTHETIC SEAWATER, -20	66	1055	200	10
NATURAL SEAWATER, -20	66	483	62.4	5

Table 10. Comparison of torque and tensile rod shear techniques. [17]

COMPARISON OF TORQUE ROD AND TENSILE ROD SHEAR TECHNIQUES	TORQUE ROD SHEAR STRESS	TENSILE ROD SHEAR STRESS
AVERAGE (kPa)	1581	1450
STANDARD DEV. (kPa)	400	203
RANGE (kPa)	1041-2917	1186-1765
NUMBER OF READINGS	40	10

Table 11. Torque adhesion of various types of ice on an alkyd coating at –20°C. [17]

TORQUE ADHESION OF VARIOUS TYPES OF ICE ON AN ALKYD COATING AT -20°C				
WATER USED	TIME (hr)	AVERAGE STRESS (kPa)	STANDARD DEV. (kPa)	NUMBER OF READINGS
BOILED, DISTILLED	2.25/4	1205	351.7	20
FRESH DISTILLED	2	712	89.5	5
FRESH DISTILLED	66	645	224.8	5
SYNTHETIC SEAWATER	3.5/6.5	166.5	69.1	10
SYNTHETIC SEAWATER	16	266.4	33.7	5
SYNTHETIC SEAWATER	66	449.5	110.7	5
NATURAL SEAWATER	6.5	77.8	52	5
NATURAL SEAWATER	66	216.4	14.2	5

Table 12. Torque adhesion of ice on various coatings and coating additives. [17]

TORQUE ADHESION OF ICE ON VARIOUS COATINGS AND COATING ADDITIVES				
COATING	ADDITIVE	AVERAGE STRESS (kPa)	STANDARD DEV. (kPa)	NUMBER OF READINGS
ALKYD		1205	351.7	20
GLOSSY ALKYD		712	89.5	5
SANDED ALKYD		2997	1274	5
ALKYD	POLYFLUO 400	541	87.4	5
ALKYD	PEG 400	683	74.9	5
MOLYKOTE No.33	AEROSIL R972	168.6	62.9	5
MOLYKOTE No.33	AEROSIL R812	33.3	13.7	5
RTV SILICONE 3-5000	AEROSIL R972	451.6	281.2	5
RTV SILICONE 1890	PEG400	56.2	7.1	5
RTV SILICONE 1890	0.5% LFC RESIN	22.9	2.9	5
LATEX 514H		1357	420	5
LATEX 514H	3.4% SLIP-AYD	664	487	5
ACRYLOID F10	6.7% SLIP-AYD 425	499	48.7	5
ACRYLOID F10	MP26	208	98	5
ACRYLOID F10	$CaCl_2$ - 85%	298	116	5
ALEFRO SIII	ALKYD	117.2	53.1	5
ALEFRO SIII	BARE ROD	59.7	39.0	5
ALEFRO FX	BARE ROD	166.5	32.7	5
LUMIFLON 100	BARE ROD	764	422	5
VELLOX 140	S76 PRIMER	248	87.2	5

Table 13. Impact test on ice produced incrementally. [17]

IMPACT TEST ON ICE PRODUCED INCREMENTALLY				
VEHICLE	ADDITIVE	ICE THICKNESS (mm)	TOTAL IMPACT (J)	RESULTS
3-5000	16% MP26	7	1.07	95% ICE REMOVED
1890	NONE	3-6	2.79	50% ICE REMOVED
1890	7.7% PEG400	7	0.23	100% ICE LOST ADHESION
1890	23% MP26	5.5	0.14	100% ICE LOST ADHESION
MOLYKOTE 33	30% R972	5	0.23	100% ICE REMOVED
MOLYKOTE 33	67% R972	7	1.39	100% ICE REMOVED
ACRYLOID F10	21% MP26	4	2.09	100% ICE REMOVED
VELLOX 140	NONE	7.5	0.23	100% ICE LOST ADHESION

Table 14. Impact test on ice produced with sprayed water. [17]

IMPACT TEST ON ICE PRODUCED WITH SPRAYED WATER				
VEHICLE	ADDITIVE	ICE THICKNESS (mm)	TOTAL IMPACT (J)	RESULTS
ALKYD	16% MP26	7	2.66	95% ICE REMOVED
ALKYD	NONE	6.5	2.84	95% ICE REMOVED
ACRYLOID F10	57.4% R792	5	2.32	LITTLE REMOVED, ICE ADHESION GOOD
ACRYLOID F10	84% ice PTFE	7	2.10	95% ICE REMOVED
1890	23% MP26	5	0.23	100% ICE REMOVED
MOLYKOTE 33	30% R972	6	0.32	100% ICE REMOVED
MOLYKOTE 33	67% R972	7	1.39	100% ICE REMOVED
ALEFRO SIII	NONE	8	2.79	95% ICE REMOVED
ALEFRO FX	NONE	6	1.07	100% ICE REMOVED
VELLOX 140	NONE	9	0.23	100% ICE REMOVED

Table 15. Composition of tested resins and additives. [17]

RESINS	COMPOSITION	COMMENTS
514H	ALKALI SOLUBLE LATEX	EASILY REMOVEABLE TOPCOAT
DOW CORNING RTV 1890	SILICONE SEALANT	WEAK, SOFT RUBBERY FILMS
DOW CORNING RTV 3-5000	SILICONE SEALANT	WEAK, SOFT RUBBERY FILMS
MOLYCOTE 33	SILICONE	FRAGILE AND POWDERY COATINGS
ACRYLOID F10	ACRYLIC	TEMPORARY COATING, EASILY REMOVABLE BY SOLVENT

ADDITIVES	COMPOSITION	COMMENTS
PTFE	POLYTETRAFLUOROETHYLENE	
MP26	HYDROPHOBIC SILICONE WAX	
PEG400	POLYETHYLENE GLYCOL	
POLYFLUO 400	MIXTURE OF POLYETHYLENE WAX AND POLYTETRAFLUOROETHYLENE	
SLIP-AYD SL425	HYDROPHOBIC SILICONE WAX	
AEROSIL R972	HYDROPHOBIC SILICA PIGMENT	
AEROSIL R812	HYDROPHOBIC SILICA PIGMENT	
LPC RESIN	WATER-SOLUBLE VINYL PYRROLIDINE RESIN	

COMMERCIAL COATINGS	COMPOSITION	COMMENTS
LUMINFLON 100	FLUORO-URETHANE	HARD SMOOTH SLIPPERY COATING
VELLOX 140	ORGANO-POLYSILOXANE	GREASY, EASILY DEFORMED
ALEFRO FX	FLUOROCARBON/SILICONE	HARD, SMOOTH, SLIPPERY
ALEFRO SIII	ORGANO-POLYSILOXANE	TRANSLUCENT, SLIPPERY WAXY
GE ANTI-FOULING	SILICONE	VERY LITTLE INFORMATION SUPPLIED BY MANUFACTURER
GE D-SS6800	URETHANE	
SANCURE 898 WITH XAMA-7	AQUEOUS URETHANE DISPERSION/POYFUNCTIONAL AZIRIDINE CATALYST	DID NOT WEATHER WELL

Table 16. Torque adhesion values for ice release coatings. [17]

TORQUE ADHESION VALUES FOR ICE RELEASE COATINGS	
COATING	TORQUE (IN-LB)
DOW CORNING RTV 1890	99.3
DOW CORNING RTV 1890 WITH MP26 WAX POWDER	29.8
MOLYKOTE #33 WITH AEROSIL R812	66.3
GENERAL ELECTRIC D-SS6800	52.2
ACRYLOID F10 WITH MP 26	82.0
ALEFRO SIII	3.5
ALEFRO SIII WITH PEG400	2.5
ALEFRO SIII WITH LFC	2.7
ALEFRO FX	6.9
SANCURE 898 WITH XAMA-7	47

Table 17. Results of ice accretion tests. [17]

RESULTS OF ICE ACCRETION TESTS				
COATING	AVERAGE WEIGHT OF ICE FORMED (lb)	RANGE OF WEIGHT OF ICE FORMED	AVERAGE # IMPACTS	AVERAGE WEIGHT OF ICE REMOVED
1. ALKYD (1-GP-61)	8.4	4.9 - 12.7	3.8	2.2
3. DOW CORNING RTV 1890 WITH MP26 WAX POWDER	11.2	10.2 - 12.9	1	11.2
4. MOLYKOTE #33 WITH AEROSIL R812	5.6	3.0 - 7.4	1.3	4.1
5. GENERAL ELECTRIC D-SS6800	8.8	6.0 - 10.2	1.7	5.3
6. GE ANTI-FOULING COATING	8.8	6.0 - 10.2	1.7	5.3
7. ACRYLOID F10 WITH MP26	5.8	3.4 - 7.4	3.3	1.7
8. ALEFRO SIII	9.1	7.4 - 10.0	1.7	5.5
9. ALEFRO SIII WITH PEG400	7.0	3.7 - 9.5	1	7.0
10. ALEFRO SIII WITH LFC	10.3	7.6 - 13.6	2	5.2
11. ALEFRO FX	11.8	11.1 - 13.2	1	11.8
12. SANCURE 898 WITH XAMA-7	7.6	7.0 - 7.9	2.7	2.8

Table 18. Effect of accelerated weathering on ice release properties. [17]

EFFECT OF ACCELERATED WEATHERING ON ICE RELEASE PROPERTIES				
	BEFORE WEATHERING		AFTER WEATHERING	
COATING	# BLOWS	RESULT	# BLOWS	RESULT
2. DOW CORNING RTV 1890	1 6 10	ICE CRACKS 20% REMOVED 20% REMOVED	1 6 10	ICE CRACKS NO REMOVAL NO REMOVAL
3. DOW CORNING RTV 1890 WITH MP26 WAX POWDER	3 6 7	20% REMOVAL 50% REMOVAL 100% REMOVAL	1 2 10	ICE CRACKS NO REMOVAL
4. MOLYKOTE #33 WITH AEROSIL R812	1 2	ICE CRACKS 100% REMOVAL, COATING DELAMINATES	1 3 6	ICE CRACKS 10% REMOVAL 100% REMOVAL, COATING DELAMINATES
5. GENERAL ELECTRIC D-556800	2 5 6	25% CRACKING 50% REMOVAL 100% REMOVAL, COATING DELAMINATES	4 6 10	100% CRACKING 5% REMOVAL 75% REMOVAL
6. GE ANTI-FOULING COATING	1 5 10	100% CRACKING 10% REMOVAL 25% REMOVAL	1 9 10	100% CRACKING 25% REMOVAL 33% REMOVAL
7. ACRYLOID F10 WITH MP26	3 4 6	25% CRACKING 50% REMOVAL 100% REMOVAL	1 3 4	25% CRACKING 50% REMOVAL 100% REMOVAL
8. ALEFRO SIII	1 3 10	5% CRACKING 10% REMOVAL 100% REMOVAL	1 10	50% CRACKING 100% CRACKING
9. ALEFRO SIII WITH PEG400	1 2 4	25% CRACKING 50% CRACKING 100% REMOVAL	1 2 4	50% CRACKING 100% CRACKING 100% REMOVAL
10. ALEFRO SIII WITH LPC	1 2 3 5	50% CRACKING 50% REMOVAL 75% REMOVAL 100% REMOVAL	1 2 3	50% CRACKING 50% REMOVAL 100% REMOVAL
11. ALEFRO FX	1 2 3 4	75% CRACKING 10% REMOVAL 50% REMOVAL 100% REMOVAL	1	100% REMOVAL
12. SANCURE 898 WITH XAMA-7	1	100% REMOVAL, COATING HAS BLASTERS BUT NO LOSS OF ADHESION	1 3 10	10% CRACKING 50% CRACKING 30% COATING DELAMINATION

8.2 Active De-icing Coating for Airfoils

An active coating [18] was developed at Dartmouth College for in-flight de-icing. When a small DC bias is applied, a small electric current electrochemically decomposes ice attached to the protected surface, consequently breaking the ice bonds. This development was based on the recent discovery that an applied DC bias, depending on the magnitude and polarity, can enhance or reduce the bond interface strength by a magnitude of one, or even eliminate it completely.

There are two mechanisms responsible for this behavior. For applied voltages of less than 2 volts, an interfacial electric double-layer is produced, thus enhancing or reducing the electrostatic part of ice adhesion. When double-layers of electric charge form, they provide a good exchange of electric charge between ice and metals. This mechanism is completely reversible. When the applied voltage is greater than 2 volts, an electrolytic gas ($2H_2 + O_2$) is then generated (see Figure

18). These bubbles act as interfacial cracks exfoliating ice from the metal. Experiments have shown that a 21V bias has reduced the bond strength by an order of one for 30-60 seconds.

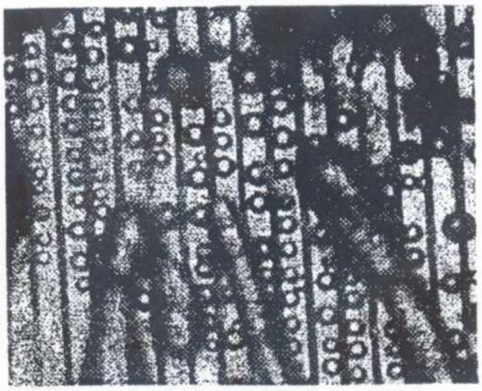

Figure 18. Electrolytic gas generated by applied voltage. [18]

A thin grid of electrodes is fabricated using a technology called photolithography. A 50X50 mm square mask was used, which consisted of 4 square unit cells. Each of these unit cells contained two comb-like grids as shown in Figure 19. A 5-µm-thick copper clad laminate was placed onto either a 125-µm flexible kapton film or epoxy resin fiberglass insulative material. The copper grids were then formed with photolithography, and followed by chemical etching. The electrodes were then electroplated with Au or Pt to enhance their resistance to electro-corrosion.

When ice forms on top of these grids, there would be two paths of current flow, either along the surface of the substrate between the anode and cathode (surface current), or up through the bulk of the ice from the anode to the cathode (bulk current) (see Figure 20). The surface conductance (G_S) and bulk conductance (G_B) can be estimated by the following equations, where b is the distance between the anode and cathode, and a is the width of the cathode and anode themselves and σ_B and σ_S are the electrical conductivity of the bulk and surface respectively.

$$G_B = \frac{\sigma_B}{3a} \qquad G_S = \frac{\sigma_S}{2a^2}$$

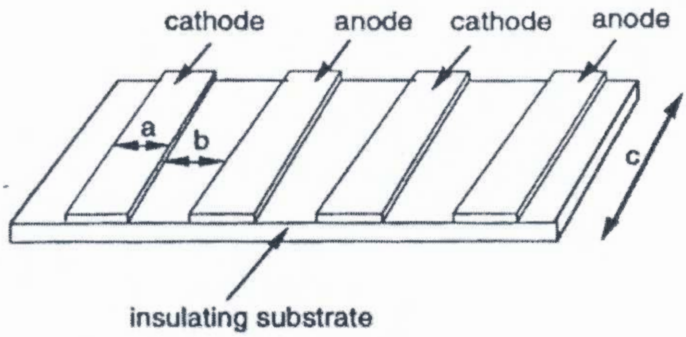

Figure 19. Schematic of grid and electrodes arrangement. [18]

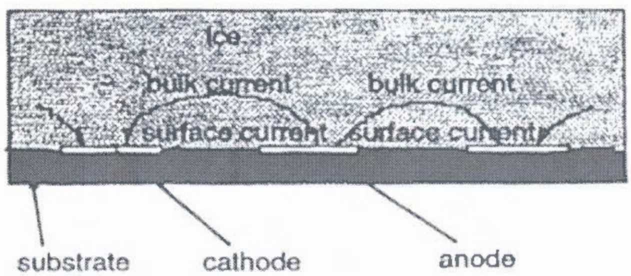

Figure 20. Bulk current travels within the ice body between the cathode and anode. Surface current travels along the ice/substrate interface between the two electrodes. [18]

From the equations, it can be seen that as a decreases, the surface conductance will increase faster than bulk. For $a \leq 1$ cm, surface conductance will dominate thus breaking ice/substrate interface bonds.

Mechanical testing was also performed to explore this principle. Shearing tests were conducted in a temperature range between -5 and -22°C. A DC bias of 5 volts was initially applied to obtain the electric double layers, and then distilled water was frozen. The voltage was then increased to 10 to 30 V, and the specimen was sheared to break load. A distinct correlation between applied voltage and adhesive shear strength was determined, as shown in Figure 21. Note: a voltage between 2V – 5V must be initially applied to form the electric double layers, otherwise the de-icing effect would be slight or absent.

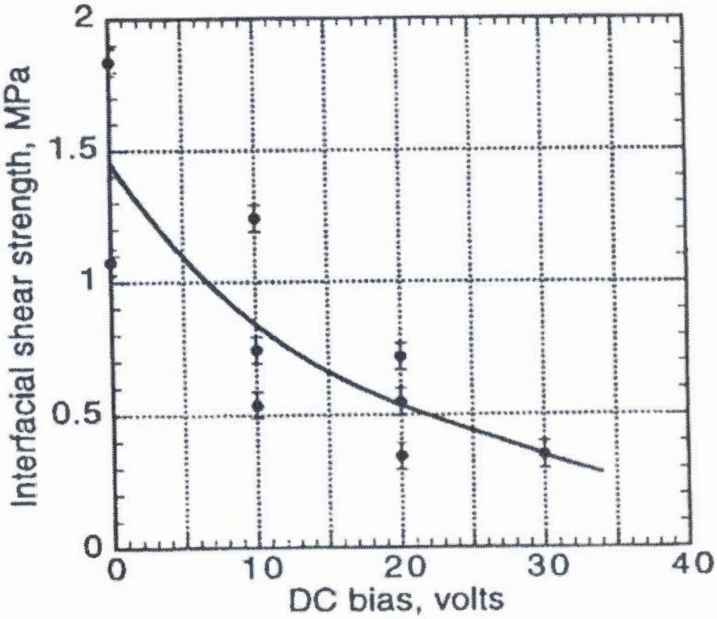

Figure 21. Shear testing results: decreasing interfacial shear strength with increasing applied voltage. [18]

Advantages	Disadvantages
• Power consumption is much lower than electro-thermal. Only 0.2 to 0.75 kW/m^2 are needed • Low weight, conceivably even lower weight than other electrical systems	• No certified applications have been known or even tested, hence minimal knowledge available • Normal rainwater may not be electrically conductive enough to support this technique. Test ice was doped to increase voltage, and the spacing between electrodes was decreased • A trace amount of impurities (1ppm) would considerably increase the voltage of ice, hence bulk conductance would increase faster than surface conductance, minimizing the current flowing along the surface and causing de-icing to be more difficult

9.0 Shape Memory Alloys

Shape memory alloys (SMA) are finding unique applications in numerous fields. Applications of SMAs are as diverse; cut lengths of wire, machined medical guide wire cores, stents, clot filters, cellular telephone antenna blanks, orthodontic arches, shaped wires for surgical instruments, trocar-pointed NiTi rods, photo chemically-etched sheet, shaped helical forms, etc. SMAs are made to perform a thermally-activated, diffusionless phase change, resulting in a change of dimension analogous to thermal expansion of typical materials, only the expansion of an SMA is at levels high enough to de-ice. Preliminary research has explored designs of actively- and a passively-powered SMA. A thermal mat would provide the activation energy in an actively-powered concept. Alternatively, a passively-powered scheme would tap into energy released during the water to ice phase change to provide the required activation energy. Both actively- and passively-activated SMA de-icing systems work on the principle that ice will form on the SMA sheet's leading edge and, with a high strain value coupled with SMA expansion or contraction, the protected surface/ice bond would be broken, allowing ice to be shed in the air stream. NiTi SMAs are particularly suitable for rotorcraft applications due to restrictions in aerodynamic intrusions (NiTi material would be a thin sheet), weight, power, and durability. The NiTi composition (usually 55% weight Ni) is also known for high erosion- and corrosion-resistance and excellent fatigue properties and it can additionally serve a dual role as a de-icer as well as a durable erosion shield.

The unique metallurgical composition of SMAs allow a very large thermally-induced shape transformation over a relatively low temperature spectrum. For example, NiTi, a common SMA, is able to exhibit up to 8% strain [19]. Due to their large internal stresses, SMAs can be designed to impart a force during the dimensional change, and therefore the SMA can act as a mechanical actuator.

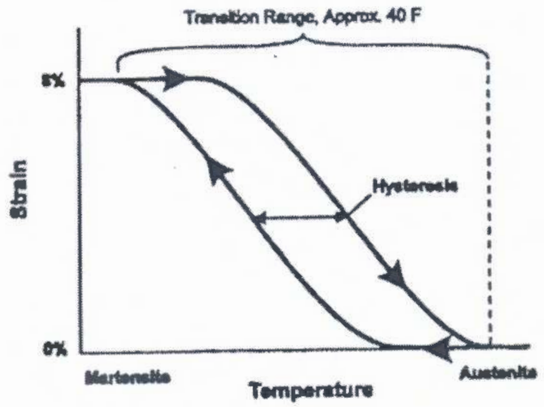

Figure 22. Thermal cycle required for martensitic to austenitic phase change for NiTi SMA. [19]

The phase cycle of the NiTi SMA is shown in Figure 23. When the material is on the cold side of the hysteresis curve, a martensitic crystallographic structure exists and is characterized for this alloy by a soft and ductile nature. At this point, it is possible to plastically strain the material up to 8% by cold working. Upon heating, the material will transform to a fully austenitic crystal structure and will exhibit a hard and inflexible nature. The ability of the material to transform itself back to its original shape upon an energy transfer (heat, magnetic) gives it the name of a shape memory alloy. For this particular NiTi alloy composition, the full-phase transition occurred over a 40°F (~22.2°C) span. Depending on the composition, the transition temperature can be tailored to occur anywhere between –350°F to 250°F (-212.2°C to 121.1°C) [19].

If the SMA is constrained from deforming back to its original shape during the heating cycle, then internal stresses in the order of 10 ksi (68.95 MPa) per percent deforming strain will develop [19], and therefore the SMA is able to produce a useful movement and force. One large problem associated with designing a SMA actuator is the pronounced hysteresis curve of Figure 22. An excessively large reversing temperature change is needed to stimulate a reversed dimensional change, and intuitively these large temperature ranges may not be possible from some SMAs.

When design calls for a NiTi high-life cycle SMA, then the maximum strain output must be limited, as inducing higher strains will disproportionably lower the life cycle capacity. At 3%, a maximum strain value was projected, allowing a maximum life cycle of 10000 cycles while producing a net stress output of 20 ksi (137.90 MPa) as the upper bounds. Wind tunnel testing at NASA's Lewis Icing Research Tunnel determined that a strain of 0.1% to 0.3% at a shear stress level of 0 to 200 psi (0 to 1.38 MPa) was required to eliminate the adhesive shear strength of ice. Therefore, the projected 3% maximum strain value, and 20 ksi (137.90 MPa) net stress output comfortably falls into these ranges, and NiTi SMA has the potential to perform ice de-bonding action [19]. With a sufficient safety factor, a 0.2% strain must be readily provided at any point of the icing spectrum, which spans over 50°F (~ 28°C). The shearing mechanism created by the SMA to de-bond the ice is illustrated in Figure 23.

Figure 23. SMA ice de-bonding mechanism. [19]

9.1 Passively Powered SMA Design:

The energy required for the contraction/expansion motion of the SMA to de-bond a sheet of ice is provided from the latent energy of heat released from the liquid to solid phase change [19]. This energy loss is transformed to available surface heat. The passively powered SMA cross section is illustrated in Figure 24.

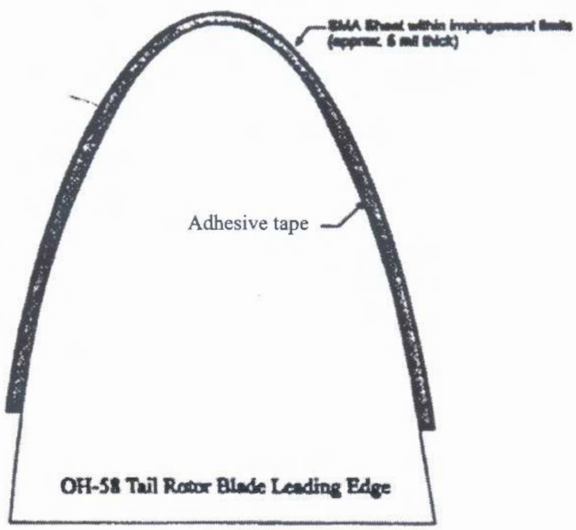

Figure 24. Passively powered SMA concept: A thin NiTi sheet is placed over leading edge and allowed to thermally deform. [19]

The passive de-icing model is demonstrated in Figure 25. During freezing, and depending on the ambient temperature, the energy released by the water is able to provide a temperature rise of up to 25°F (13.8°C) followed by a decrease in temperature as the surface returns to ambient. Note that as the ambient temperature approaches 32°F (0°C), this temperature-rise event will decrease in magnitude. The icing surface temperature vs. time for 5 different ambient temperatures is plotted in Figure 26. If a de-icing event is initiated at the maximum point of this temperature rise, an additional rise is experienced due to the freezing of the next layer of water, assuming that the first layer is de-bonded. This rise will be followed by a rapid decrease, however if another de-bonding event is initiated at the same point as the previous (the trough of the sinusoidal wave type), then a saw-tooth heat cycle develops, which in effect is a potential heat cycle to power an SMA. As mentioned earlier, the attainable temperature range, is a function of the ambient temperature and if freezing occurs near 32°F (0°C), an electro-thermal heater mat would then be necessary to provide the supplemental heating. Even though an auxiliary heater is necessary, it would operate on a partial cycle basis, and theoretically would still save energy as compared to a fully electro-thermal system.

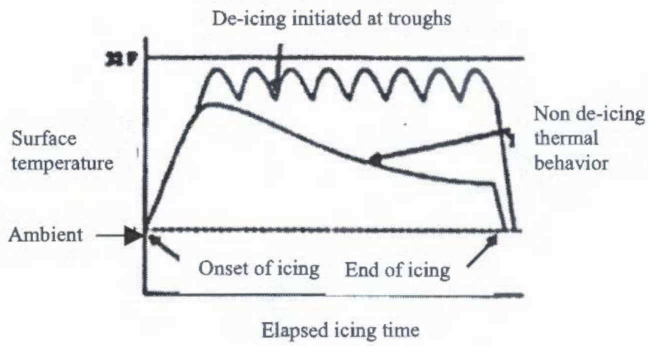

Figure 25. SMA passively-powered operation principle. [19]

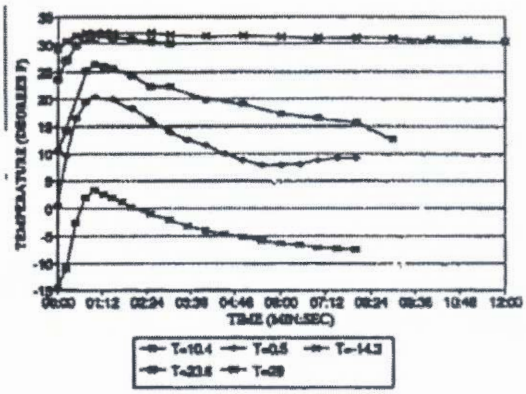

Figure 26. Temperature vs. Time curves: Temperature at the ice/substrate interface recorded against time for 5 different samples frozen at different ambient temperatures. Note lower the ambient temperature, the more that the pronounced temperature ranges experienced. [19]

A practical SMA de-icing material must have a small hysteresis width, otherwise excessively large reverse temperatures may be needed to overcome the hysteresis, and these ranges are not always possible. By varying composition, material processing, and design loading, the transition temperature, hysteresis width, and available stress and strain output can be tailored. More research is necessary to optimize a SMA for a passively powered operation; however, if properly controlled, this phenomenon could automatically prevent ice adhesion to rotating wing surfaces.

Actively-Powered SMA Design:

In order to de-ice, an SMA actively-powered actuator will pull on an icing surface which exhibits good elastic properties and imparting sufficient shearing forces to sever ice from the sheet [19], (see Figure 27). The actuator portion consists of the SMA material, an electro-thermal heater mat to provide the energy necessary for the expansion/contraction motion required, and some insulation. The icing surface area must be sufficiently elastic, and also exhibit uniform strain behavior to ensure that all regions of the sheet stretch evenly.

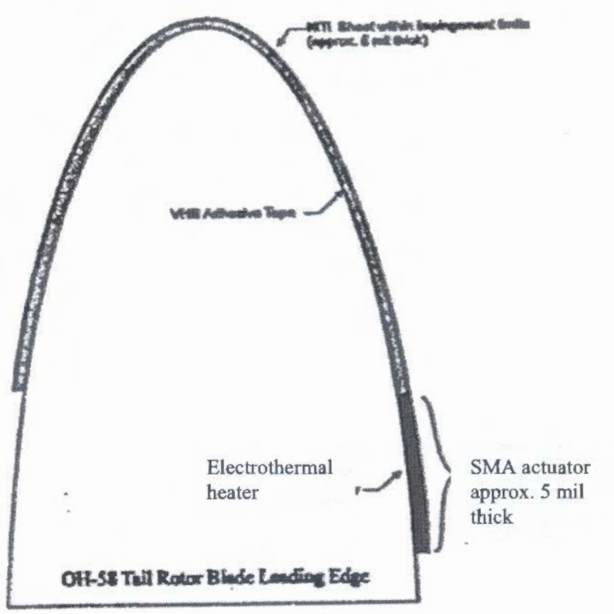

Figure 27. Actively-powered SMA concept cross section. A NiTi erosion sheet integrated to a NiTi SMA actuator. [19]

The investigated transition temperature range was from 120°F to 160°F (48.9°C to 71.1°C). This was chosen to ensure that the de-icer would not self-initiate, since the temperature range is above the projected flight envelope. Due to the high temperature, however, the SMA actuator must be sufficiently isolated and insulated well from the icing surface. No heat should be lost to the icing surface, as this energy would assist in melting the ice, allowing the efficiency to fall to that comparable of current electro-thermal systems. Due to the heaters, the problem of providing large reverse temperatures to satisfy the hysteresis is no longer an issue.

An added design concern now falls into the difficulty of joining the SMA to a sufficiently elastic icing surface. Adhesive bonding may be unreliable at high temperatures, and riveting would result in increased bulk and weight. Realizing that NiTi itself is a very elastic, and corrosion-, erosion-, and abrasion-resistant material, it would be an excellent candidate for both the SMA actuator and the icing surface. After heavy cold working, NiTi alloys exhibit high elasticity values required for the erosion shield and, following a localized heat treatment upon a portion of the NiTi alloy, a SMA actuator can be produced. A process developed by IDI was able to incorporate the NiTi actuator and the NiTi icing surface into a single sheet.

Full-scale wind tunnel tests on an OH-58 (NACA 0012 airfoil) at temperatures down to -40°F (-40°C), with rotation speeds of 1350rpm and wind speeds of 90mph (40.2 m/s), were conducted. Evidence was shown that ice thicknesses of 1/8 inch (3.2 mm) could be de-bonded and shed at a centrifugal force of 700g while ice of 3/16" (4.76 mm) could be de-iced at 100g. Therefore, in order to de-bond using an SMA de-icer, minimum ice thickness of 1/8" (3.2 mm) must be present from the blade tip to mid-span, and 3/16" (4.76 mm) from mid-span to blade root. Any ice thickness less than 1/8" (3.2 mm) could not be de-iced at the rotational speeds tested. Prior to testing, small quantities of residual ice did remain, it was smaller or comparable to other mechanical or thermal de-icing systems [20].

In order for SMAs to be a practical tool in de-icing, considerable research must still be done. Future work includes:

1. Optimizing the SMA for optimum stress and strain output
2. Reducing temperature hysterisis
3. Tailoring transition temperature to occur over full icing spectrum (if possible)
4. Developing SMA de-icers for rotor blade installation

Advantages	Disadvantages/Limitations
• Power savings: SMA required 500 Joules of energy, while electrothermal required 5000 Joules of energy for the same de-iced region during a 60-	• Early development stage, very minimal experience with de-icing application • Research needed to obtain an SMA with practical thermal range properties

second span [19] • Estimated weight of an actively powered SMA de-icing system would be approximately 100lbs (80% that of an electro-impulse de-icing system • SMA de-icing system would consume an order of magnitude less power than electro-thermal de-icing systems (1-3 kW) • Erosion, corrosion, and abrasion resistance of NiTi alloys: possible to act as an erosion shield • No practical patent yet, one patent exists but cannot de-ice sufficiently well • Very light weight • Possibility of operating with no applied power • SMA actuators produce up to 100 times more force per unit weight compared to piezoelectric actuators	• Difficulty in designing an actuator, icing sheet mechanism built from shape sheet

10.0 Summary

This literature review identified seven technologies that could potentially be used for rotorcraft blade de-icing. The literature review found few technologies that demonstrate potential in terms of practicality, acceptable aerodynamic penalties, and cost effectiveness. Two of the technologies, electro-thermal and fluid, are currently used in flight operations and an additional two; pneumatic boots and electro-vibratory, have either seen limited in-flight testing or have been tested on a blade test rig. Any new technologies must consume an order of magnitude less power then the electro-thermal de-icing system, while limiting overall cost and weight. Electro-vibratory and EIDI are promising due to their low power consumption and effectiveness; however, the complexity of their designs when adapted to rotor blades, creates a concern as it may be impossible to implement properly. So far, the blade boots have caused an unacceptable increase in vibratory loads, a problem that will be difficult to overcome. Fluid anti-icing is not aerodynamically intrusive, but its de/anti-icing time is limited to the amount of liquid onboard and fluid availability. The performance aspects of several conventional de-icing systems are summarized in Table 19. Coatings are favorable in terms of operating with no aerodynamic penalties, as well as requiring no pilot intervention; however, a coating with the adequate weatherability and durability properties needed to operate in the severe environment of rotor blade icing is yet to be developed. Shape memory alloys represent a very promising approach due to their proven use as powerful actuators. With the combination of being very lightweight, possessing excellent weatherability properties, and the possibility of operating with little or no power supplied from the aircraft shape memory alloys are a preferred option.

Table 19. Weight, power required, aerodynamic penalty, and run back potential summary of several de-icing systems.

	Electro-Thermal	Fluid	Pneumatic	Electro-Impulse	Vibratory	Shape Memory Alloy
Weight (lb)	162	194	54	120	120	100
Electrical power required (kW)	26	Negligible	Negligible	1.0	1.3	1.0
Performance effects	19% Torque Rise	No Penalty	27% Torque Rise	10% Torque Rise	10% Torque Rise	No Penalty
Runback potential	Yes	No	No	No	No	No

11.0 References

1. Ramanathan S, Varadan VV, Varadan VK (2000) "De-icing for helicopter blades using piezoelectric actuators", Smart structures and materials 2000 - Smart electronics and MEMS; Proceedings of the Meeting, Newport Beach, CA, Mar. 6-8, 2000 (A00-39382 10-31)

2. Spriggs, J.T. (1988), "An Ice Detection System for Helicopters", AIAA/IEEE Digital Avionics Systems Conference, 8th, San Jose, CA, Oct. 17-20, 1988, Technical Papers

3. Thomas S.K., Cassoni R.P., MacArthur C.D., (1996), "Aircraft Anti-icing and De-icing Techniques and Modeling", AIAA, Aerospace Sciences Meeting and Exhibit, 34th, Reno, NV, Jan. 15-18, 1996, AIAA Paper 96-0390

4. Cansdale, J T; Gent, R W; Dart, N P (2000), "The role of analysis in the development of rotor ice protection systems", European Rotorcraft Forum, 26th, Sept 26-29, 2000, Proceedings. Vol. 2 (A01-20808 04-05), Amsterdam, Netherlands, National Aerospace Laboratory, 2000, p. 97.1-97.11

5. Coffman, H.J, JR (1987), "Helicopter Rotor Icing Protection Methods", American Helicopter Society Journal, Vol. 32, pp. 34-39

6. Scavuzzo R. J., Chu M.L., Kellackey C.J. (1990), "Impact Ice Stresses In Rotating Airfoils", 28th Aerospace Sciences Meeting, Reno, Nevada, January 8-11, 1990

7. "Electrothermal Systems". DOT/FAA/CT-88/8-2. Chapter III Section 2.0, August 2001

8. Sirotinkskij, Boris S. (1993), "Blade Anti-Icing Systems for Mil Helicopters", European Rotorcraft Forum, 19th, Como, Italy, September 14-16, 1993, Proceedings Vol. 1.

9. "Conventional Pneumatic Boot Systems". DOT/FAA/CT-88/8-2. Chapter III Section 1.0, August 2001

10. Wiesend N.A. Jr. (1988), "Design of an Advanced Pneumatic De-Icer for the Composite Rotor Blade", AIAA 26th Aerospace Sciences Meeting, Reno, Nevada, January 11-14, 1998

11. Hindel James T, Weisend Norbet A. (1991) "Low energy ice protection for helicopters" European Rotorcraft Forum, 17th, Berlin, Germany, Sept. 24-26, 1991, Paper. 12 p.

12. "Pneumatic Impulse De-icing Systems". DOT/FAA/CT-88/8-2. Chapter III Section 1.0A, February 2002

13. "Fluid Ice Protection Systems". DOT/FAA/CT-88/8-2. Chapter III Section 3.0 August 2001

14. "Electro-Impulse De-Icing Systems". DOT/FAA/CT-88/8-2. Chapter III Section 4.0, February 2002

15. Zumwalt G.W., Friedberg R.A (1986), "Designing an Electro-Impulse De-Icing System", AIAA 24th Aerospace Sciences Meeting, Reno, Nevada, January 6-9, 1986, AIAA-86-0545.

16. http://www.idiny.com/abstracts/amceia.html

17. Foster Terry (1993), "Investigation of Novel Ice Release Coatings", Proceedings Rotary-Wing Aircraft In-Flight Icing/De-icing Workshop, Ottawa, June 1993

18. Petrenko, Victor F.l Courville, Zoe (2000). "Active De Icing Coating for Aerofoils". AIAA, Aerospace Sciences Meeting and Exhibit, 38th Reno, NV. Jan. 10-13 2000

19. Gerardi R.B, Ingram, R.A, (1995), "Shape memory alloy based de-icing system for aircraft" AIAA, Aerospace Sciences Meeting and Exhibit, 33rd, Reno, NV, Jan. 9-12, 1995, AIAA Paper 95-0454

20. Gerardi J.J., Ingram R.B., Catarella R.A. (1995), "Wind Tunnel Test Results For a Shape Memory Alloy Based De-icing System For Aircraft", American Helicopter Society International Icing Symposium '95, Montreal, Canada, September 18-21, 1995

21.http://meted.ucar.edu/icing/pcu6/pcu6web/index.htm